


Above the weak nonlinearity: super-nonlinear waves in astrophysical and laboratory plasmas

Alexander E. Dubinov^{1,2} · Dmitrii Y. Kolotkov³ 

Received: 1 September 2017 / Accepted: 10 January 2018 / Published online: 1 February 2018
© Division of Plasma Physics, Association of Asia Pacific Physical Societies 2018

Abstract The review summarises recent theoretical achievements and observational manifestations of a new, recently discovered type of nonlinear oscillations in multi-component plasmas, namely super-nonlinear periodic waves and super-nonlinear solitary waves (supersolitons). Both are characterised by a non-trivial topology of their phase portraits, highly anharmonic profile shapes, extremely long periods, and large amplitudes. Based upon multi-fluid magnetohydrodynamic plasma models, examples of ion-acoustic and Alfvén super-nonlinear waves are considered. A multi-component nature of the plasma was revealed to be a crucial condition for the existence of these super-nonlinear waves, with the complexity of the system growing with the number of plasma species accounted for in the model. A minimum number of plasma components which allow for the existence of super-nonlinear waves are also discussed. From the observational point of view, typical signatures of periodic super-nonlinear waves are manifested, for example, in the oscillatory processes operating in the magnetised plasma of the solar corona and ground-based plasma machines. Super-nonlinear solitary structures (supersolitons) of an electrostatic origin are recognised in the Earth’s magnetosphere, laboratory experiments with chemically active plasmas, and numerical simulations.

Keywords Super-nonlinear wave · Supersoliton · Multi-component plasma

✉ Dmitrii Y. Kolotkov
d.kolotkov@warwick.ac.uk

Alexander E. Dubinov
dubinov-ae@yandex.ru

¹ Sarov Institute for Physics and Technology, Sarov, Nizhny Novgorod Region, Russia 607188

² National Research Nuclear University “MEPhI”, Moscow, Russia 115409

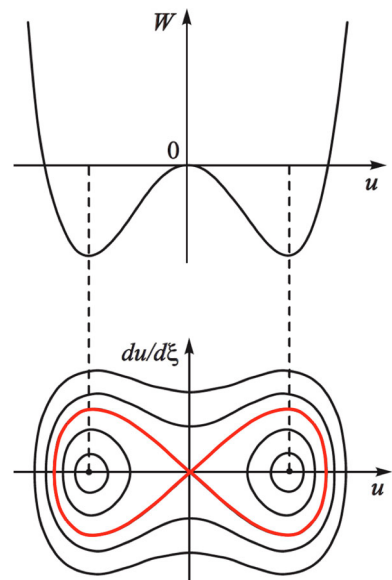
³ Department of Physics, Centre for Fusion, Space and Astrophysics, University of Warwick, Coventry CV4 7AL, UK

1 Introduction

The physical quantity u experiencing oscillations of a constant amplitude in a periodic wave is well known to correspond to a closed trajectory without self-intersections in a phase plane (\dot{u}, u) . A total phase portrait of the wave, characterising the whole dynamical system, is represented by a family of such phase trajectories nested one in another and surrounding the point of a stable equilibrium (also often referred to as a *centre*). Small amplitude trajectories in the phase portrait, concentrated in the vicinity of the equilibrium point, correspond to small amplitude harmonic oscillations of the quantity u . Their oscillation properties, such as a typical period and phase speed, can be determined with a standard linearisation technique and subsequent analysis of the linearised governing equations. On the other hand, the presence of closed trajectories in the phase portrait indicates the existence of an invariant energy in the dynamical system, also referred to as a generalised potential energy, which has a minimum coinciding with the position of the stable equilibrium point. This formalism is applicable for both the conservative and non-conservative systems (see, e.g. the closed phase trajectories in Chin et al. 2010).

However, such a trivial topology of the phase portrait of periodic waves is not unique. For example, the phase portrait containing a special phase trajectory, separatrix, is shown in the bottom plot of Fig. 1 (Ryskin and Trubetskov 2000). In this portrait, the outermost phase trajectories enveloping the separatrix correspond to highly nonlinear periodic waves, whose total energy is above a certain potential barrier height and the amplitude cannot be smaller than that of the separatrix. Based on these facts, Ryskin and Trubetskov (2000) called these stationary large-amplitude waves as super-nonlinear waves (SNWs). They also proposed a particular

Fig. 1 Effective potential energy, $W(u)$, and the corresponding phase diagram of stationary solutions of the modified Korteweg–de Vries equation (1). A special phase trajectory, separatrix, is indicated by the red line (adapted from Ryskin and Trubetskov 2000)



example of the commonly known modified Korteweg–de Vries (mKdV) equation, which accounts for the effects of a cubic nonlinearity and has the periodic stationary solutions of a super-nonlinear type:

$$u_t + u^2 u_x + \beta u_{xxx} = 0, \quad (1)$$

where β is a positive constant coefficient. The stability of these mKdV waves, including super-nonlinear regimes, was investigated by Murawski (1987) on the basis of the *Infeld–Rowlands* method (Infeld and Rowlands 2000). In particular, the authors found that super-nonlinear mKdV solutions can be stable in a certain range of their oscillation amplitudes. In addition to the mKdV equation (1), other particular examples of classical low-dimensional nonlinear oscillators, whose effective potential energy has two stable equilibria and thus supports super-nonlinear regimes, are the Duffing equation and the derivative nonlinear Schroedinger equation (see, e.g. Lopes et al. 2014; Hada et al. 1989, where these equations were employed for the modelling of the 11-year solar cycle and nonlinear Alfvén waves and solitons in astrophysical plasma systems, respectively). According to the definition of SNWs given by Ryskin and Trubetskov (2000), the generalised potential energy of the oscillating system must have at least two minima separated by a single maximum, to support the existence of SNWs (see, e.g. Fig. 1). In this configuration of the generalised energy, the points of the local minima correspond to the positions of stable equilibria (*centres*), while the maximum point, where the separatrix intersects itself, shows the unstable equilibrium, also known as a *saddle* point. One can conclude that the presence of several maxima and minima in the generalised potential energy most likely indicates the ability of the system to sustain SNWs in a periodic or even solitary form.

Due to their unique properties, such as large amplitudes, long periods, and highly anharmonic profile shapes (see Sect. 2.1 for details), SNWs are certainly among the most intriguing extreme phenomena in real physical systems, and the question of whether they can be detected, in particular, in space and laboratory plasmas attracts a growing interest in the research community. A comprehensive analysis of the previous studies dealing with nonlinear waves of various types in plasmas reveals that there are a number of works where the generalised potential energy (hereafter the *Sagdeev* or *Bernoulli* pseudopotentials) was found to have two or even three local minima. For example, Kuehl and Imen (1985) and Cairns et al. (1995) obtained the pseudopotential of the ion-acoustic waves in the electron–ion plasma, which may have two minima under certain physical conditions. More specifically, for the existence of a double-well pseudopotential in these models the electron plasma component must have an essentially non-thermal distribution, which allows the electrons to be separated into several groups of different energies. Similar properties of the pseudopotential energy were found for the electrostatic waves propagating in the electron–positron plasma (Verheest et al. 1996), where both plasma components were taken to consist of cold and hot populations. Another interesting example of two minima appearing in the pseudopotential is of the oblique electrostatic waves in the magnetised four-component plasma with cold and hot electrons and heavy and light ions, as shown in Ghosh and Lakhina (2004) in the

application to the auroral regions of the Earth's magnetosphere. Additionally, ion-acoustic and dust-acoustic modes in dusty plasmas of various models may also have a pseudopotential energy with two minima (see, e.g. Choi et al. 2007; Dubinov and Sazonkin 2008, 2013; Baluku et al. 2010; Akbari-Moghanjoughi 2010; Mamun and Shukla 2010; Dubinov et al. 2011; Verheest 2011 for recent studies). The pseudopotential with two minima also appears in the analyses of electrostatic waves in magnetised electron–positron–ion plasmas (Ansar Mahmood et al. 2005), and in the magnetised electron–ion plasma with two oppositely charged ion components (Kaur and Singh Gill 2010). Three minima in the pseudopotential energy for nonlinear dust-acoustic waves in an electron–ion plasma with negatively and positively charged dusty grains, were found in Verheest (2009). This particular example implies an even more complicated topology of the phase portrait of the wave, with two separatrices, one of which fully envelops the other. Hence, a broader set of (*super-*)nonlinear solutions can be naturally expected in this case. We also need to mention that in addition to electrostatic waves in plasmas, the magneto-hydrodynamic (MHD) waves can have multi-well pseudopotentials too. For example, Choi and Lee (2007) and Masood et al. (2010) analysed the propagation of Alfvén waves in a dusty plasma addressing magnetospheric and laboratory plasma structures and self-gravitating molecular clouds, and found the corresponding pseudopotentials with two minima. In all the studies listed above, periodic solutions of the SNW type are possible. However, none of these works consider waves with amplitudes larger than that of separatrices. It is the purpose of the present review to rectify this omission.

By studying the details of the plasma models in the above examples, which allow the potential energy to contain several minima, we emphasise the importance of a multi-component nature of the plasma. Indeed, an obvious correlation of the number of plasma species taken into account in a model with the complexity of the potential energy topology and the nonlinear wave forms, appearing in such a plasma, most likely exists. The latter in turn seems to be a crucial condition for the identification of SNWs in plasma systems, which indicates that only multi-component plasmas are able to support super-nonlinear periodic solutions. Such multi-species plasmas can be adequately described by the multi-fluid approaches that have been widely used in space physics and aeronomy (see, e.g. Schunk 1977; Barakat and Schunk 1982 and all the references mentioned in the above paragraph). In particular, such multi-fluid models of the plasma are intensively developed in the application to lower layers of the Earth's magnetosphere (e.g. Konikov et al. 1989; Demars and Schunk 1994; Ganguli 1996) and solar wind (e.g. Echim et al. 2011; Abbo et al. 2016).

On the other hand, the special phase trajectories, separatrices, are known to correspond to essentially nonlinear solutions describing the evolution of shock waves, double layers, and solitons in plasma. Hence, as a natural extension of the basic idea of periodic SNWs, one can assume the case, when there are several separatrices in the phase portrait, and one of them fully envelops the others (see, e.g. Verheest 2009). Similar to periodic SNWs, this outermost separatrix corresponds to a new super-nonlinear type of solitary waves in plasma, which can be referred to as a *supersoliton*. According to such a definition, the supersolitons represent a group of solitary SNWs that combines the unique properties of solitary structures and

extreme characteristics of SNWs. So far, the concept of supersolitons became commonly accepted among researchers and is extensively developed in a number of recent works (see, e.g. Hellberg et al. 2013; Maharaj et al. 2013; Verhees et al. 2013a, b, c, 2014; Dutta et al. 2014; Ghosh and Sekar Iyengar 2014; Lakhina et al. 2014; Rufai et al. 2014, 2015, 2016a; Verheest et al. 2014; Verheest 2014; Olivier et al. 2015; Rufai 2015; Singh and Lakhina 2015; Verheest and Hellberg 2015; Paul and Bandyopadhyay 2016 and Sect. 3.3 for details). In the present review we focus on the results obtained in the pioneer studies of periodic SNWs (Dubinov et al. 2011, 2012) and supersolitons (Dubinov and Kolotkov 2012b, c; Dubinov et al. 2012a) in multi-component plasmas typical for astrophysical and laboratory conditions. We also demonstrate several observational examples of these super-nonlinear structures detected in the plasma of the solar atmosphere, Earth's magnetosphere, laboratory and numerical experiments.

2 Super-nonlinear waves (SNWs)

2.1 Classification and signatures of periodic SNWs

Different oscillatory physical processes have different topologies of their phase portraits, characterised by a certain number of stable equilibrium points (*centres*) and by a number of special phase trajectories, separatrices, which additionally may vary in shape. In particular, Fig. 2 schematically illustrates the examples of the phase portraits with 2, 3, and 4 centres and several layers of separatrices. The complexity of the phase portraits naturally grows with the complexity of the oscillating system, where the discussed super-nonlinear waves (SNWs) always represent the most non-trivial cases.

Following the recipe proposed by Dubinov et al. (2012), various forms of SNWs could be classified according to the topology of their phase portraits as $\text{SNW}_{m,n}$, where m is a number of centres embedded within the SNW phase trajectory and n is a number of separatrices enveloped by this trajectory. For example, in a basic case when the oscillating system has only two stable equilibria (see panel (a) in Fig. 2), large amplitude $\text{SNW}_{2,1}$ with the phase trajectories located above a single separatrix, are allowed. In a more complicated scenario when there are three stable equilibria in the system, the phase portrait can have two essentially different configurations (see b, c in Fig. 2), with $\text{SNW}_{3,1}$, and $\text{SNW}_{3,2}$ and $\text{SNW}_{2,1}$, respectively. A variety of topologically different phase diagrams appears in systems with four stable equilibria (d–g in Fig. 2), thus straightforwardly leading to a much richer set of super-nonlinear solutions. Additionally, we need to mention that all the portraits shown in Fig. 2 support the existence of ordinary stationary nonlinear waves, $\text{NW}_{1,0}$ known as cnoidal waves, whose phase trajectories are concentrated around each separate centre, and are restricted in amplitude by the nearest separatrix. However, the aspects of their evolution are out of the scope of the present review and are not considered further.

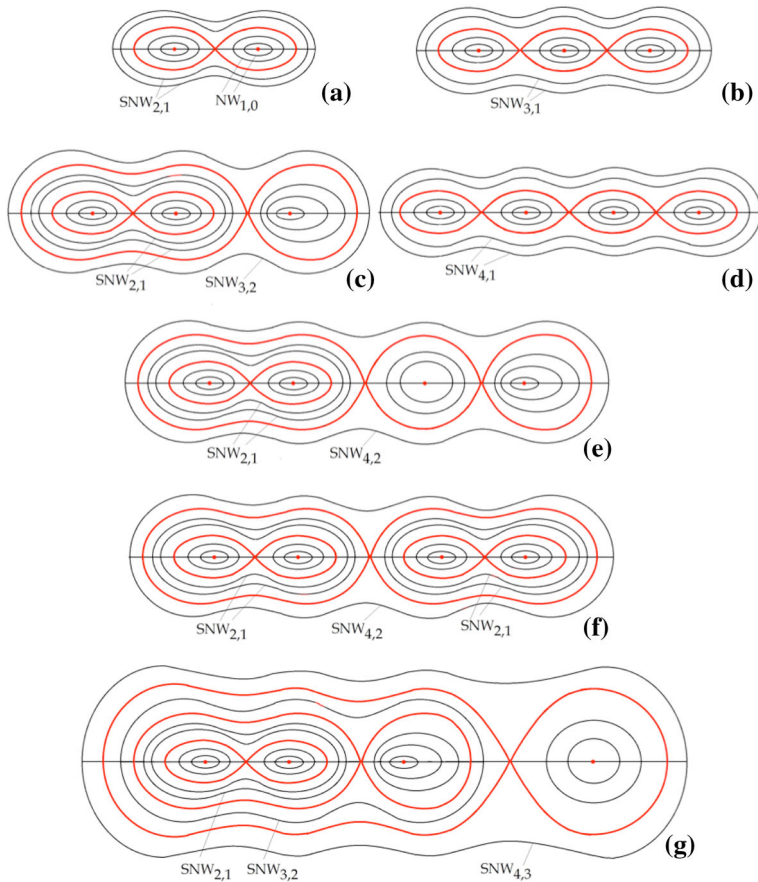


Fig. 2 Sketch showing the classification of super-nonlinear waves (SNWs) by the topology of their phase portraits with 2 (a), 3 (b, c), and 4 (d–g) stable equilibrium points (*centres*). Separatrices are indicated by the red lines in each phase portrait (adapted from Dubinov et al. 2012)

We now describe the unique signatures of SNWs, allowing for the distinguishing of them among the whole possible oscillating ensemble detected in observations. By definition, these are essentially large-amplitude fluctuations, with typical amplitudes which are sufficiently higher than the background level. Their profiles are always anharmonic, of a symmetric triangular shape, with at least four points appearing in a single oscillation cycle, where the second derivative is equal to zero. Due to such anharmonicity and their original super-nonlinear nature, the Fourier spectral analysis of SNWs shows the appearance of well-pronounced equidistant higher harmonics in a power spectrum provided the noise level is sufficiently low. However, traditional spectral techniques based upon Fourier transforms and wavelets are known to use a priori assigned harmonic basis functions, and, hence, are obviously limited in the analysis of such highly anharmonic signals, as SNWs. Instead, a novel Hilbert–Huang Transform (HHT) spectral method has recently been developed for the analysis of such nonlinear signals (Huang et al. 1998, 2008). It

uses the empirical mode decomposition (EMD) technique, which expands the signal of interest into a basis derived directly from the data, iteratively searching for the local timescales naturally appearing in the signal. Hence, due to its adaptive nature, the HHT spectral technique is essentially suitable for the processing of highly nonlinear anharmonic time series typical for SNWs.

Another interesting property of SNWs is related to their temporal evolution, namely in the case where the oscillating system dissipates the energy and SNWs decay, their amplitude decreases gradually until a specific value which corresponds to the amplitude of the nearest separatrix. After that, a very rapid decrease (on the timescale shorter than the oscillation period) of the oscillation amplitude most likely occurs, accompanied by the transformation of the wave type (for example, from SNW_{3,2} to SNW_{2,1}, as illustrated in Fig. 2). Such sudden changes of the oscillation amplitude can be detected in observations. Similarly, in the opposite case of the continuous energy supply or an instability development in the system, the amplitude of SNWs may increase rapidly when it reaches the upper separatrix level, providing the corresponding change of the wave type (for example, from SNW_{2,1} to SNW_{3,2} or from SNW_{3,2} to SNW_{4,3}, according to Fig. 2). In the following sections we consider a number of distinct examples of various multi-fluid magnetohydrodynamic plasma models which lead to the possibility of periodic SNWs.

2.2 Ion-acoustic periodic SNW_{2,1} in a plasma with two oppositely charged ions

As the first illustration we show that the periodic solutions of an ion-acoustic SNW_{2,1} type can exist in a three-species plasma with electrons and two oppositely charged ion components. The plasma is assumed to be uniform, collisionless, and unmagnetised.

For the unperturbed initial state of such a plasma the full neutrality condition can be written as $Z_1 n_{0i1} - Z_2 n_{0i2} - n_{0e} = 0$, where $e < 0$ is the electron charge, $(-Z_1 e) > 0$ is the electric charge of the positive ions, and $Z_2 e < 0$ is the electric charge of the negative ions. Hereafter, all variables with the subscript “1” refer to the positively charged ion component, while the subscript “2” corresponds to the negative ions. Introducing the dimensionless parameters of the model: $\alpha = n_{0i2}/n_{0i1}$, $\beta = m_{i2}/m_{i1}$, and $v = \sqrt{m_{i1} V^2/kT_e}$, where V is the phase speed of the propagating ion-acoustic wave and k is the Boltzmann constant, the initial neutrality condition reduces to $n_{0e} = n_{0i1}(Z_1 - \alpha Z_2)$. We also assume the temperature of both ion components to be sufficiently low, allowing for the neglecting of the ion thermal pressure in the model, while the electrons are taken to be hot and inertialess, governed by the Boltzmann distribution:

$$n_e = n_{0e} \exp\left(-\frac{e\phi}{kT_e}\right). \tag{2}$$

It should be noted here that the neglect of the electron inertia as used in the Hall plasma approximation is not always valid. Example of oblique travelling wave solutions for whistler *oscillitons* in which the electron momentum can be of the

same order as that of the protons is described in Webb et al. (2008). However, the further consideration of such higher frequency effects is out of the scope of this review, and is not addressed in the following discussion.

The set of hydrodynamic equations governing the dynamics of the ion components in the wave is

$$\frac{\partial n_{i1,2}}{\partial t} + \frac{\partial(n_{i1,2}v_{i1,2})}{\partial x} = 0, \quad (3)$$

$$\frac{\partial v_{i1,2}}{\partial t} + v_{i1,2} \frac{\partial v_{i1,2}}{\partial x} = \pm \frac{Z_{1,2}e}{m_{i1,2}} \frac{\partial \varphi}{\partial x}, \quad (4)$$

$$\frac{\partial^2 \varphi}{\partial x^2} = 4\pi e(Z_1 n_{i1} - Z_2 n_{i2} - n_e), \quad (5)$$

where in the equation of motion (4) plus/minus corresponds to the positive/negative ions, respectively.

Large-amplitude stationary ion-acoustic waves in such a formulation are now analysed with the use of the mechanical analogy approach based on the Sagdeev pseudopotential (Davidson 1972). The wave is assumed to propagate in the positive direction of the x -axis with the phase speed V . Introducing the variable $\xi = x - Vt$ in Eqs. (2)–(5) and assuming all quantities to be functions of ξ only, so that

$$\frac{\partial}{\partial t} = -V \frac{d}{d\xi}, \quad \frac{\partial}{\partial x} = \frac{d}{d\xi}, \quad (6)$$

one changes the frame of reference to that travelling with the phase speed of the perturbation, V . In addition, when transforming to this new frame, the velocity of both ion components in the wave should be also modified according to the Galilean transformation rule,

$$u_{i1,2} = v_{i1,2} - V. \quad (7)$$

In the transformation (7), v_i is the velocity of the ion plasma component in the laboratory frame, where the unperturbed plasma is at rest, and u_i is the corresponding velocity in the frame of reference related to the wave, where the unperturbed plasma moves in the opposite direction of the x -axis, with the speed V . Equations (2)–(5) now reduce to

$$\frac{d(n_{i1,2}u_{i1,2})}{d\xi} = 0, \quad (8)$$

$$u_{i1,2} \frac{du_{i1,2}}{d\xi} = \pm \frac{Z_{1,2}e}{m_{i1,2}} \frac{d\varphi}{d\xi}, \quad (9)$$

$$\frac{d^2 \varphi}{d\xi^2} = 4\pi e(Z_1 n_{i1} - Z_2 n_{i2} - n_e). \quad (10)$$

Integrating the continuity equations (8) and the equations of motion (9) with the initial conditions $n_{i1,2} = n_{0i1,2}$, $\varphi = 0$, and $u_{i1,2} = -V$, one obtains the explicit dependence of the ion concentrations $n_{i1,2}$ upon the electrostatic potential φ as

$$n_{i1,2} = n_{0i1,2} \left(1 \pm \frac{2Z_{1,2}e\varphi}{m_{i1,2}V^2} \right)^{-1/2}. \tag{11}$$

The subsequent substitution of Eqs. (2) and (11) into the Poisson’s equation (10) results in

$$\frac{d^2\varphi}{d\xi^2} = 4\pi\rho(\varphi), \tag{12}$$

where

$$\begin{aligned} \rho(\varphi) = & Z_1en_{0i1} \left(1 + \frac{2Z_1e\varphi}{m_{i1}V^2} \right)^{-1/2} \\ & - Z_2en_{0i2} \left(1 - \frac{2Z_2e\varphi}{m_{i2}V^2} \right)^{-1/2} - n_{0e} \exp\left(-\frac{e\varphi}{kT_e}\right). \end{aligned}$$

Treating φ and ξ as a generalised coordinate and time of a pseudoparticle, second-order ordinary differential equation (12) has a form of the equation of motion of a particle in the force field $4\pi\rho(\varphi)$. Furthermore, in its first integral written as

$$\frac{1}{2} \left(\frac{d\varphi}{d\xi} \right)^2 + U_S(\varphi) = \text{const}, \tag{13}$$

the second term on the left-hand side represents a generalised potential energy of the particle, often referred to as the Sagdeev pseudopotential, $U_S(\varphi)$. In Eq. (13) $U_S(\varphi)$ is given by

$$\begin{aligned} U_S(\varphi) = & -4\pi \int_0^\varphi \rho(\varphi) d\varphi = 4\pi m_{i1}V^2 \left\{ n_{0i1} \left[1 - \left(1 + \frac{2Z_1e\varphi}{m_{i1}V^2} \right)^{1/2} \right] \right. \\ & \left. + n_{0i2} \frac{m_{i2}}{m_{i1}} \left[1 - \left(1 - \frac{2Z_2e\varphi}{m_{i2}V^2} \right)^{1/2} \right] + n_{0e} \frac{kT_e}{m_{i1}V^2} \left[1 - \exp\left(-\frac{e\varphi}{kT_e}\right) \right] \right\}, \end{aligned} \tag{14}$$

where the constant of integration on the right-hand side of Eq. (13) represents the total energy of the particle and depends only on the initial conditions. The minimum of function (14) corresponds to the initial equilibrium (full electrical neutrality) of the unperturbed plasma with $\varphi = 0$.

We recall that by definition, this plasma model is able to support periodic ion-acoustic solutions of the SNW type when the pseudopotential energy (14) has at least two local minima. Hence, the values of the dimensionless parameters of the model, providing such a configuration of the function U_S , are chosen. Figure 3 shows that the latter is possible for both $V < V_s$ and $V > V_s$ cases, where

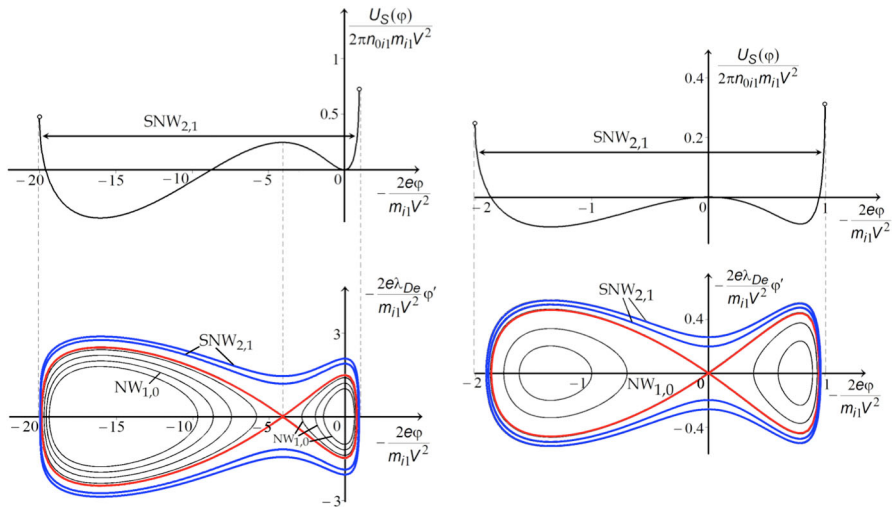


Fig. 3 Left: pseudopotential $U_S(\varphi)$ given by Eq. (14) and the phase portrait of a subsonic ion-acoustic wave in a plasma with two oppositely charged ion components plotted for $\alpha = 0.1$, $\beta = 20$, $\nu = 0.7$, $Z_1 = 1$, and $Z_2 = 1$. Right: pseudopotential $U_S(\varphi)$ given by Eq. (14) and the phase portrait of a supersonic ion-acoustic wave in a plasma with two oppositely charged ion components plotted for $\alpha = 0.3$, $\beta = 2$, $\nu = 1.6$, $Z_1 = 1$, and $Z_2 = 1$. Separatrices and super-nonlinear phase trajectories of the $SNW_{2,1}$ type are indicated by the red and blue lines, respectively, in each phase portrait (adapted from Dubinov et al. 2012)

$V_s = (kT_e/n_{0e})^{1/2}(Z_1^2n_{0i1}/m_{i1} + Z_2^2n_{0i2}/m_{i2})^{1/2}$ is the ion-sound speed in the plasma, obtained from the dispersion relation of the linear theory describing the oscillations in the vicinity of $\varphi = 0$ (see, e.g. Dubinov 2009). In other words, both subsonic (left-hand column of Fig. 3) and supersonic (right-hand column of Fig. 3) SNW periodic solutions are possible.

More specifically, both pseudopotentials U_S shown in Fig. 3 are found to contain two local minima, guaranteeing the existence of a periodic ion-acoustic SNW in the analysed three-species plasma, which can be classified as $SNW_{2,1}$ according to the scheme described in Sect. 2.1. Their phase trajectories are illustrated in the bottom plots of Fig. 3 among the whole phase portraits of the dynamical system governed by Eq. (12). Highly anharmonic profiles of the normalised electrostatic potential φ , obtained from numerical solutions of Eq. (12) and periodically varying in the revealed subsonic and supersonic $SNW_{2,1}$, are shown in Fig. 4.

We also need to mention that in addition to the discussed extremely large amplitude $SNW_{2,1}$, the potential functions and phase portraits shown in Fig. 3 imply the existence of stationary solutions in the form of ordinary smaller amplitude nonlinear waves, $NW_{1,0}$ known as cnoidal waves. Their phase trajectories in turn envelop each separate *centre* in the phase portraits. However, those $NW_{1,0}$ solutions whose trajectories do not correspond to the initial equilibrium of the unperturbed plasma with $\varphi = 0$ (namely the trajectories enveloping the left-hand *centre* in the phase portrait of the subsonic case and all $NW_{1,0}$ solutions obtained in the supersonic regime) should be disregarded.

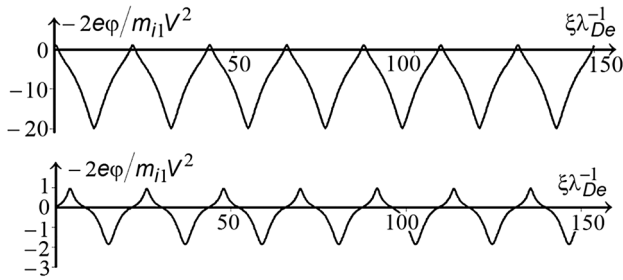


Fig. 4 Top: variations of the electrostatic potential φ in a subsonic ion-acoustic SNW_{2,1} (plotted with the same set of parameters as shown in Fig. 3, left-hand column) in a plasma with two oppositely charged ion components. Bottom: variations of the electrostatic potential φ in a supersonic ion-acoustic SNW_{2,1} (plotted with the same set of parameters as shown in Fig. 3, right-hand column) in a plasma with two oppositely charged ion components (adapted from Dubinov et al. 2012)

This example confirms the possibility for the existence of the SNW_{2,1} periodic solutions of an ion-acoustic type in a three-species plasma containing the hot Boltzmann electrons and two oppositely charged cold ion components. It also allows one to formulate straightforward empirical criteria resulting from the analysis of the pseudopotential function $U_S(\varphi)$, which in turn can be rewritten also in terms of the plasma parameters (e.g. the ratio of the concentrations of different species, their temperatures, and characteristic velocities) and need to be rigorously satisfied for the existence of SNWs in a dynamical system:

- The first derivative of a pseudopotential function $U_S(\varphi)$, which is in fact an effective generalised force governing the dynamics of a pseudoparticle, must have at least two real roots, that results in a double-well form of the pseudopotential;
- The edge points (shown with the blank circles in Fig. 3) of the interval where $U_S(\varphi)$ has real values, must be above the local maximum of the function $U_S(\varphi)$, separating its two local minima.

2.3 Electrostatic periodic SNW_{2,1}, SNW_{3,1}, and SNW_{3,2} in a four-species plasma

Consider a more complex model of the plasma consisting of four components: hot electrons and positrons, and two cold ion species with opposite electric charges. Similar to the previous section, the initial full electrical neutrality condition for the unperturbed state of such a plasma is $Z_1en_{0i1} - Z_2en_{0i2} - en_{0e} + en_{0p} = 0$, where an additional term en_{0p} describing the positron contribution appears. Introducing again the dimensionless parameters of the model, as $\alpha = n_{0i2}/n_{0i1}$, $\beta = m_{i2}/m_{i1}$, $\delta = n_{0p}/n_{0i1}$, $\tau = T_p/T_e$, and $v = \sqrt{m_{i1}V^2/kT_e}$, where V and k are the phase speed of the electrostatic wave propagating in the plasma and the Boltzmann constant, respectively, the initial neutrality condition can be rewritten as $n_{0e} = n_{0i1}(Z_1 - \alpha Z_2 + \delta)$.

Based on the multi-fluid description of the plasma, the dynamics of the cold ion components in the ion-acoustic wave is governed by Eqs. (3)–(4) with the Poisson's law having the form

$$\frac{\partial^2 \varphi}{\partial x^2} = 4\pi e(Z_1 n_{i1} - Z_2 n_{i2} - n_e + n_p). \quad (15)$$

The set of Eqs. (3)–(4) and (15) is complemented by the Boltzmann law for the electron concentration (2) and the following Boltzmann distribution for positrons, which, in the spirit of the previously discussed model, are assumed to be hot and inertialess:

$$n_p = n_{0p} \exp\left(\frac{e\varphi}{kT_p}\right). \quad (16)$$

Performing the calculations, which are identical to those described in detail in Eqs. (6)–(13) of Sect. 2.2, one can derive the pseudopotential U_S as a function of the electrostatic potential φ , as

$$\begin{aligned} U_S(\varphi) = & -4\pi \int_0^\varphi \rho(\varphi) d\varphi = 4\pi m_{i1} V^2 \left\{ n_{0i1} \left[1 - \left(1 + \frac{2Z_1 e\varphi}{m_{i1} V^2} \right)^{1/2} \right] \right. \\ & + n_{0i2} \frac{m_{i2}}{m_{i1}} \left[1 - \left(1 - \frac{2Z_2 e\varphi}{m_{i2} V^2} \right)^{1/2} \right] + n_{0e} \frac{kT_e}{m_{i1} V^2} \left[1 - \exp\left(-\frac{e\varphi}{kT_e}\right) \right] \\ & \left. + n_{0p} \frac{kT_p}{m_{i1} V^2} \left[1 - \exp\left(\frac{e\varphi}{kT_p}\right) \right] \right\}, \end{aligned} \quad (17)$$

where

$$\begin{aligned} \rho(\varphi) = & Z_1 e n_{0i1} \left(1 + \frac{2Z_1 e\varphi}{m_{i1} V^2} \right)^{-1/2} - n_{0e} \exp\left(-\frac{e\varphi}{kT_e}\right) \\ & - Z_2 e n_{0i2} \left(1 - \frac{2Z_2 e\varphi}{m_{i2} V^2} \right)^{-1/2} + n_{0p} \exp\left(\frac{e\varphi}{kT_p}\right). \end{aligned}$$

Figures 5 and 6 show the pseudopotential $U_S(\varphi)$ (17) and the phase portraits of the ion-acoustic wave propagating in a four-species plasma plotted for various sets of the dimensionless parameters of the model. The pseudopotential U_S is clearly seen to have three local minima, which indicates the ability of this plasma model to support periodic ion-acoustic waves of the SNW_{2,1}, SNW_{3,2} (Fig. 5), and SNW_{3,1} (Fig. 6) types. In the obtained configurations of $U_S(\varphi)$, the position of the initial equilibrium and full electrical neutrality of the plasma correspond to either its central local minimum in the subsonic regime (Fig. 5, left-hand column) or to the right-hand local maximum in the supersonic regimes shown in the right-hand column of Figs. 5 and 6.

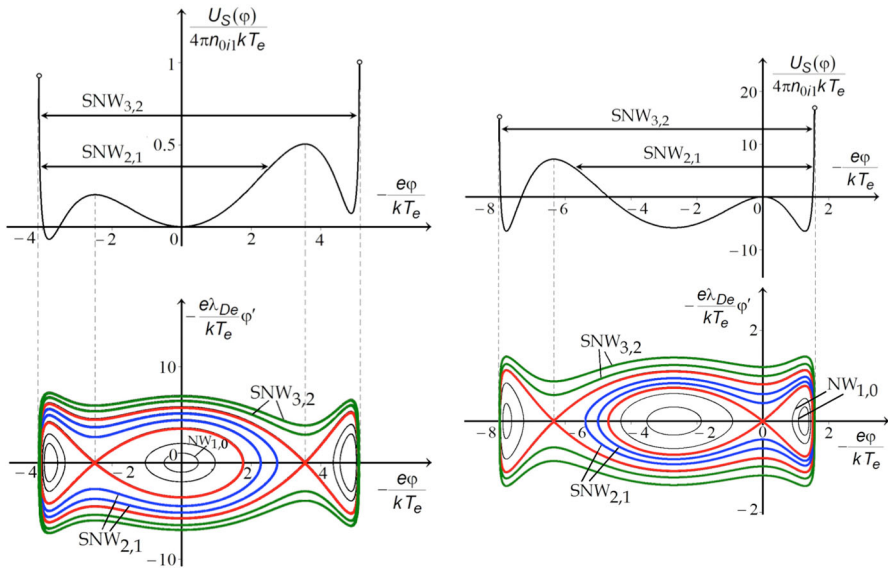


Fig. 5 Left: pseudopotential $U_S(\varphi)$ given by Eq. (17) and the phase portrait of a subsonic ion-acoustic wave in a four-species plasma plotted for $\alpha = 0.52, \beta = 1.6, \nu = 3.2, \delta = 0.07, \tau = 1, Z_1 = 1,$ and $Z_2 = 2$. Right: pseudopotential $U_S(\varphi)$ given by Eq. (17) and the phase portrait of a supersonic ion-acoustic wave in a four-species plasma plotted for $\alpha = 4.9, \beta = 0.495, \nu = 11.36, \delta = 0.044, \tau = 1, Z_1 = 41,$ and $Z_2 = 4$. In each phase portrait, separatrices are shown by the red lines; phase trajectories of periodic SNW_{2,1} and SNW_{3,2} are shown by the blue and green lines, respectively (adapted from Dubinov et al. 2012)

Variations of the electrostatic potential φ in the revealed ion-acoustic SNW_{2,1}, SNW_{3,1}, and SNW_{3,2} propagating in a four-species plasma are shown in Fig. 7. Their profiles are essentially anharmonic of a symmetric triangular shape with large amplitudes. In contrast to the previous case (see Sect. 2.2), where only SNW_{2,1} was detected in a three-species plasma model, the present example shows a broader selection of SNWs. The latter clearly illustrates an obvious correlation between the number of plasma components in the model and the variety of super-nonlinear solutions which can be expected to exist in such a plasma.

2.4 Shear Alfvén SNW_{2,1} in a four-species magnetised plasma

In addition to the electrostatic nature (see Sects. 2.2 and 2.3), SNWs may be of an electromagnetic origin too, and it is worth searching for them, for example, among plasma magnetohydrodynamic waves. For illustration, in this section the relevant model of super-nonlinear large-amplitude and high-frequency shear Alfvén waves propagating in a multi-component magnetised plasma is considered. The developed model can be attributed to the class of models investigating the contribution of high-frequency oscillatory phenomena in the solar atmosphere (with typical periods shorter than one second) to the heating of the solar corona and acceleration of the solar wind. They may be driven, for example, by various micro-turbulences and

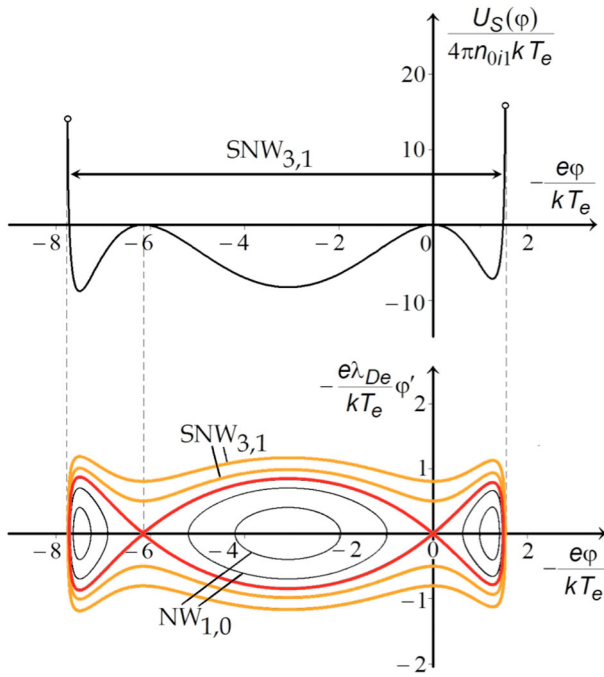


Fig. 6 Pseudopotential $U_S(\varphi)$ given by Eq. (17) and the phase portrait of a supersonic ion-acoustic wave in a four-species plasma plotted for $\alpha = 4.7$, $\beta = 0.48$, $\nu = 11.36$, $\delta = 0.0485$, $\tau = 1$, $Z_1 = 412$, and $Z_2 = 4$. Separatrix and phase trajectories of periodic $SNW_{3,1}$ are shown by the red and yellow lines, respectively (adapted from Dubinov et al. 2012)

spontaneous magnetic reconnection occurring in the photospheric–chromospheric magnetic network (Axford and McKenzie 1992; Tu and Marsch 1997), or by nonlinear cascading from lower frequencies in the corona (Isenberg and Hollweg 1983; Tu 1987).

In the model the plasma is assumed to be of an identical composition as considered in Sect. 2.3, with hot and inertialess electrons and positrons, and two sorts of cold massive ion components. The external magnetic field \mathbf{B}_0 is directed along the z -axis. The plasma is taken to be sufficiently magnetised with the plasma parameter $\beta \ll 1$ that allows one to neglect the ion thermal pressure and the ion velocity components parallel to \mathbf{B}_0 . Perturbing the plasma in the x -direction, consider a 2.5D shear Alfvén wave propagating in the xoz -plane. The schematic sketch illustrating the geometry of the problem is shown in Fig. 8. Following the assumption of a low β plasma, the electromagnetic field in the wave is determined according to the two potentials formalism (see, e.g. Chen et al. 2000; Choi and Lee 2007), with $E_x = -\partial\varphi/\partial x$, and $E_z = -\partial\psi/\partial z \equiv -\partial\varphi/\partial z - c^{-1}\partial A_z/\partial t$, where A_z is a magnetic vector potential directed along the external magnetic field \mathbf{B}_0 and c is the speed of light.

Under the simplifying assumptions described above, the transverse dynamics of the ion plasma components in the wave is governed by the following set of magnetohydrodynamic equations:

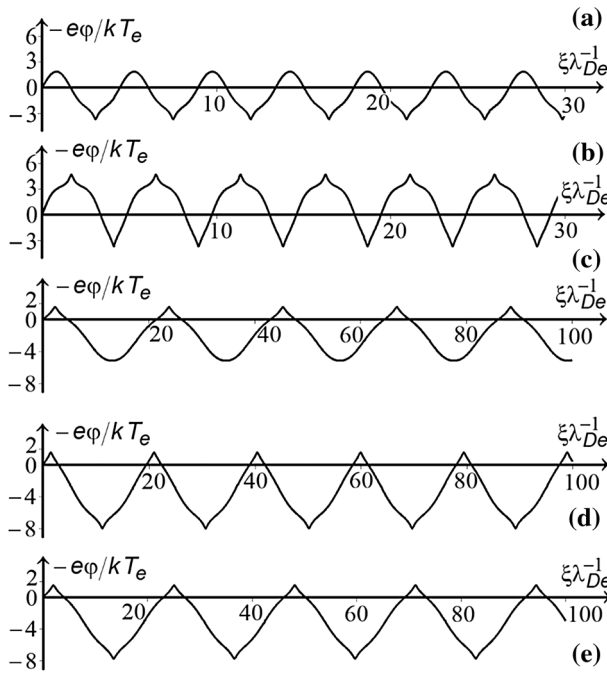
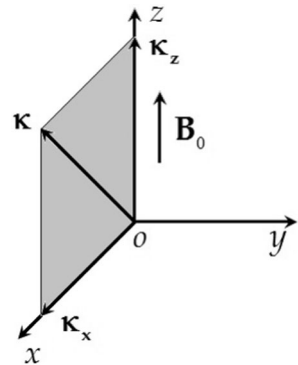


Fig. 7 **a, b** Variations of the electrostatic potential φ in a subsonic ion-acoustic SNW_{2,1} (**a**) and SNW_{3,2} (**b**) (plotted with the same set of parameters as shown in Fig. 5, left-hand column) in a four-species plasma. **c, d** Variations of the electrostatic potential φ in a supersonic ion-acoustic SNW_{2,1} (**c**) and SNW_{3,2} (**d**) (plotted with the same set of parameters as shown in Fig. 5, right-hand column) in a four-species plasma. **e** Variations of the electrostatic potential φ in a supersonic ion-acoustic SNW_{3,1} (plotted with the same set of parameters as shown in Fig. 6) in a four-species plasma (adapted from Dubinov et al. 2012)

Fig. 8 Schematic sketch illustrating the geometry of a 2.5D shear Alfvén wave in a low β plasma



$$\frac{\partial n_{i1,2}}{\partial t} + \frac{\partial(n_{i1,2}v_{i1,2x})}{\partial x} = 0, \tag{18}$$

$$\frac{\partial v_{i1,2x}}{\partial t} + v_{i1,2x} \frac{\partial v_{i1,2x}}{\partial x} = \pm \left[-\Omega_{i1,2}v_{i1,2y} + \frac{e}{m_{i1,2}}E_x \right], \tag{19}$$

$$\frac{\partial v_{i1,2y}}{\partial t} + v_{i1,2x} \frac{\partial v_{i1,2y}}{\partial x} = \pm \Omega_{i1,2} v_{i1,2x}, \quad (20)$$

where $\Omega_{i1,2} = eB_0/m_{i1,2}c$ are the cyclotron frequencies of the ion plasma components, the plus/minus signs in Eqs. (19) and (20) refer to the negative/positive ions, respectively, and the ion charge numbers $Z_1 = Z_2 = 1$.

Electrons and positrons in turn are assumed to be hot and inertialess, and hence are distributed in the wave according to the Boltzmann law written with respect to the scalar potential ψ :

$$n_e = n_{0e} \exp\left(-\frac{e\psi}{kT_e}\right), \quad (21)$$

$$n_p = n_{0p} \exp\left(\frac{e\psi}{kT_p}\right) = n_{0p} n_{0e}^\tau n_e^{-\tau}, \quad (22)$$

where the dimensionless parameter $\tau = T_p/T_e$.

Additionally, the quasi-neutrality assumption is applied to the plasma:

$$n_{i1} + n_p - n_{i2} - n_e = 0, \quad (23)$$

which reduces to $n_{0e} = n_{0i1}(1 - \alpha + \delta)$, where $\alpha = n_{0i2}/n_{0i1}$ and $\delta = n_{0p}/n_{0i1}$ are the dimensionless parameters of the initial unperturbed state of the plasma.

From equations of motion (19) and (20) one can derive the ion polarisation drift velocities, as

$$v_{i1,2x} = \pm \frac{m_{i1,2}c^2}{eB_0^2} \frac{\partial E_x}{\partial t}, \quad (24)$$

where plus/minus corresponds to the negative/positive ions, respectively.

From Maxwell's equations one obtains an expression for the parallel current density, j_z

$$\frac{\partial^4}{\partial x^2 \partial z^2} (\varphi - \psi) = \frac{4\pi}{c^2} \frac{\partial^2 j_z}{\partial t \partial z}. \quad (25)$$

Taking into account the continuity equations (18) and the quasi-neutrality condition (23), Eq. (25) can be rewritten as

$$\frac{\partial^4}{\partial x^2 \partial z^2} (\varphi - \psi) = -\frac{4\pi e}{c^2} \frac{\partial^2 (n_e - n_p)}{\partial t^2}. \quad (26)$$

Combining Eqs. (18) and (24) results in

$$\frac{\partial n_{i1,2}}{\partial t} = \pm \frac{\partial}{\partial x} \left(\frac{n_{i1,2} m_{i1,2} c^2}{eB_0^2} \frac{\partial^2 \varphi}{\partial x \partial t} \right), \quad (27)$$

where plus/minus corresponds to the negative/positive ions, respectively. Introducing a new variable

$$\xi = x + z - Vt, \quad \frac{\partial}{\partial x} = \frac{\partial}{\partial z} = \frac{d}{d\xi}, \quad \frac{\partial}{\partial t} = -V \frac{d}{d\xi}, \tag{28}$$

where V is the phase speed of the propagating wave, Eq. (27) reduces to

$$\frac{dn_{i1,2}}{d\xi} = \pm \frac{d}{d\xi} \left(\frac{n_{i1,2} m_{i1,2} c^2}{e B_0^2} \frac{d^2 \varphi}{d\xi^2} \right). \tag{29}$$

Integrating Eq. (29) with the initial conditions $\xi = 0, n_{i1,2} = n_{0i1,2}$, and $\varphi = 0$, one can derive an explicit relation between the ion concentrations in the wave, n_{i1} and n_{i2} :

$$n_{i2} = n_{0i2} \frac{n_{i1}}{n_{i1}(1 + \gamma) - \gamma n_{0i1}}, \tag{30}$$

where $\gamma = m_{i2}/m_{i1}$. Substituting Eq. (30) into the quasi-neutrality condition (23), rewrite it with respect to n_{i1} :

$$n_{i1} = \frac{1}{2(1 + \gamma)} \left[n_{0i2} + \gamma n_{0i1} - (1 + \gamma)(n_p - n_e) + \sqrt{D} \right], \tag{31}$$

where $D = [(1 + \gamma)(n_p - n_e) - n_{0i2} - \gamma n_{0i1}]^2 + 4\gamma(1 + \gamma)n_{0i1}(n_p - n_e)$. Then substituting n_{i1} (31) into the once-integrated Eq. (29) and accounting for Eq. (22), one can obtain an explicit dependence of the second derivative $d^2\varphi/d\xi^2$ upon the electron concentration n_e , which is used in further calculations:

$$\frac{d^2 \varphi}{d\xi^2} = \frac{2n_{0i1}(1 + \gamma) e B_0^2 (m_{i1} c^2)^{-1}}{n_{0i2} + \gamma n_{0i1} - (1 + \gamma)(n_p - n_e) + \sqrt{D}} - 1. \tag{32}$$

Writing the variable (28) in Eq. (26), the latter takes the form

$$\frac{d^4}{d\xi^4} (\varphi - \psi) = -4\pi e \left(\frac{V}{c} \right)^2 \frac{d^2(n_e - n_p)}{d\xi^2}, \tag{33}$$

which can be twice integrated with the initial conditions $\xi = 0, \varphi = 0, \psi = 0$, and $n_{e,p} = n_{0e,p}$, to give

$$\frac{d^2 \varphi}{d\xi^2} - \frac{d^2 \psi}{d\xi^2} = -4\pi e \left(\frac{V}{c} \right)^2 (n_e - n_p + n_{0p} - n_{0e}). \tag{34}$$

Condition (21) allows one to obtain an explicit dependence $\psi(n_e)$, written as

$$\psi = -\frac{kT_e}{e} \ln \left(\frac{n_e}{n_{0e}} \right). \tag{35}$$

Finally, substituting Eqs. (22), (32), and (35) into Eq. (34), we obtain the following second-order ordinary differential equation with respect to the function $n_e(\xi)$:

$$f(n_e) \frac{d^2 n_e}{d\xi^2} + \frac{df(n_e)}{dn_e} \left(\frac{dn_e}{d\xi} \right)^2 = g(n_e), \tag{36}$$

where the functions $f(n_e)$ and $g(n_e)$ are determined as

$$f(n_e) = \frac{d\psi(n_e)}{dn_e} = -\frac{kT_e}{e} \frac{1}{n_e}, \quad (37)$$

$$g(n_e) = \frac{eB_0^2}{m_{i1}c^2} \left[\frac{2n_{0i1}(1+\gamma)}{n_{0i2} + \gamma n_{0i1} - (1+\gamma)(n_p - n_e) + \sqrt{D}} - 1 \right] + 4\pi e \left(\frac{V}{c} \right)^2 (n_e - n_p + n_{0p} - n_{0e}), \quad (38)$$

with the function D given in Eq. (31).

Using a standard reduction of order technique, one can reduce the second-order Eq. (36) to a first-order Bernoulli differential equation with respect to the function $P(n_e) = dn_e/d\xi$, whose integral has the form of Eq. (13) with the generalised potential energy function referred to as the Bernoulli pseudopotential, $U_B(n_e)$:

$$U_B = - \int_{n_{0e}}^{n_e} f(n_e)g(n_e) dn_e. \quad (39)$$

More details about the analysis of nonlinear waves in multi-component plasmas with the Bernoulli pseudopotential technique can be found in Dubinov (2007a, b), Dubinov et al. (2010, 2011), and in references therein. Theory of highly nonlinear oscillations of current sheets generated by coalescing plasmoids has recently been developed in Kolotkov et al. (2016), with the use of the Bernoulli pseudopotential. Additionally, the Bernoulli pseudopotential method was used for the analysis of nonlinear oscillations in self-gravitating quantum plasmas and in two- and three-dimensional graphene-like fluids (Akbari-Moghanjoughi 2013, 2014).

Figure 9 shows the pseudopotentials $U_B(n_e)$ (39) and the phase portraits of a shear Alfvén wave propagating in a low-beta four-species plasma plotted for various sets of the dimensionless parameters of the model. The present configurations of U_B exhibit two local minima, which indicate the ability of the plasma to support the propagation of periodic Alfvén SNW_{2,1}. The initial neutrality of the unperturbed plasma in the examples shown in Fig. 9 may correspond to the local minimum of U_B (left-hand column of Fig. 9) or to its local maximum (right-hand column of Fig. 9). Stationary variations of the electron concentration n_e in the detected periodic Alfvén SNW_{2,1} are illustrated in Fig. 10. We would like to point out that in contrast to the linear small amplitude case, in the discussed super-nonlinear regime the Alfvén mode is essentially compressive, with extremely large amplitudes (typically comparable to the initial unperturbed background value or even higher) and anharmonic triangular profiles.

Although there are a few indirect observational evidences of the presence of a non-negligible positron fraction in the solar corona (see, e.g. Shar et al. 2004; Fleishman et al. 2013; Murphy et al. 2014), one should admit that the developed model is still sufficiently far from the actual coronal conditions. Nevertheless, its findings suggest the need for a similar analysis of a pure coronal case. For example, a background thermal plasma penetrated by the energetic electron, proton and alpha particle beams could be considered.

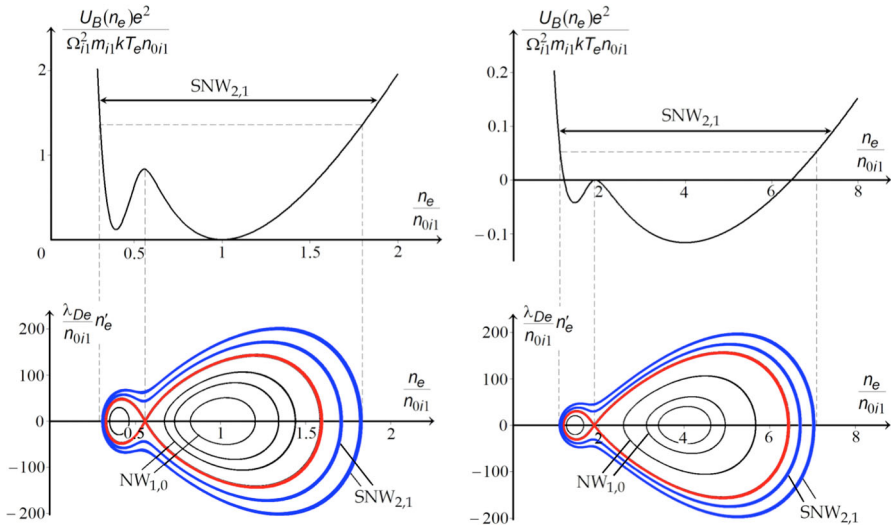


Fig. 9 Pseudopotential $U_B(n_e)$ given by Eq. (39) and the phase portrait of a shear Alfvén wave in a four-species plasma plotted for $\alpha = 0.1$, $\gamma = 0.07$, $\sqrt{m_{i1} V^2/kT_e} = 2500$, $\delta = 0.1$, $\tau = 3$, $\omega_{i1}/\Omega_{i1} = 0.01$, and $kT_e/m_{i1}c^2 = 0.01$ (left-hand column); and for $\alpha = 0.1$, $\gamma = 2$, $\sqrt{m_{i1} V^2/kT_e} = 500$, $\delta = 1$, $\tau = 3$, $\omega_{i1}/\Omega_{i1} = 0.01$, and $kT_e/m_{i1}c^2 = 0.01$ (right-hand column). The colour scheme is identical to that used in Fig. 3 (adapted from Dubinov et al. 2012)

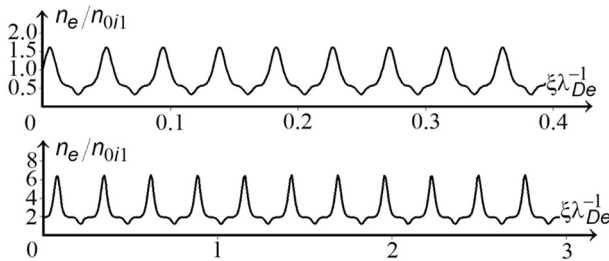


Fig. 10 Variations of the electron concentration n_e in a shear Alfvén $SNW_{2,1}$ in a four-species plasma plotted for the same set of parameters as shown in Fig. 9, left-hand column (top plot) and in Fig. 9, right-hand column (bottom plot) (adapted from Dubinov et al. 2012)

3 Solitary SNW in plasma: supersolitons

As a natural extension of the original idea of periodic super-nonlinear waves, proposed in Dubinov et al. (2011, 2012) and described in detail in Sect. 2, whose phase trajectories envelop at least one separatrix loop, one can imagine the case, where there are several separatrix layers in the phase portrait, and one of them fully envelops the others (see, e.g. schematic examples shown in (c) and (e–g) of Fig. 2). In that case the outermost separatrix represents a new form of a large-amplitude solitary wave in a system, which may be referred to as a *supersoliton*. Similar to periodic SNWs, for the existence of supersolitons in a dynamical system its

generalised potential energy must contain several (at least three) local minima separated by two local maxima. For the latter condition to be fulfilled in the electrically active medium, such as a plasma, its multi-component nature is of a crucial importance. In the following sections we demonstrate a few analytical examples of electrostatic waves in the form of supersolitons, propagating in multi-component plasmas of various hydrodynamic models. Clear agreement between theoretical solutions and observational records obtained in laboratory experiments, indicating the possibility of the existence of supersolitons in real plasmas, is also achieved.

3.1 Supersolitons in *epii*-plasma

As a first example, the most trivial model of an unmagnetised, collisionless, and uniform plasma supporting the existence of supersolitons and consisting of four charged species: namely hot and inertialess electrons “*e*” and positrons “*p*”, and cold and massive positively “1” and negatively “2” charged ion components is considered. Such a composition of the plasma is identical to that discussed in Sect. 2.3, where the periodic SNW_{2,1}, SNW_{3,1}, and SNW_{3,2} of an electrostatic origin were studied. Similar to the analysis performed in Sect. 2.3, we write the initial full electrical neutrality condition for the unperturbed state of such a four-species plasma, as $Z_1 en_{0i1} - Z_2 en_{0i2} - en_{0e} + en_{0p} = 0$, where the subscript “0” refers to the parameters of the initial equilibrium of the plasma, $e < 0$ is the electron charge, $(-e) > 0$ is the positron charge, and $(-Z_1 e) > 0$ and $Z_2 e < 0$ are the electric charges of the positive and negative ions, respectively.

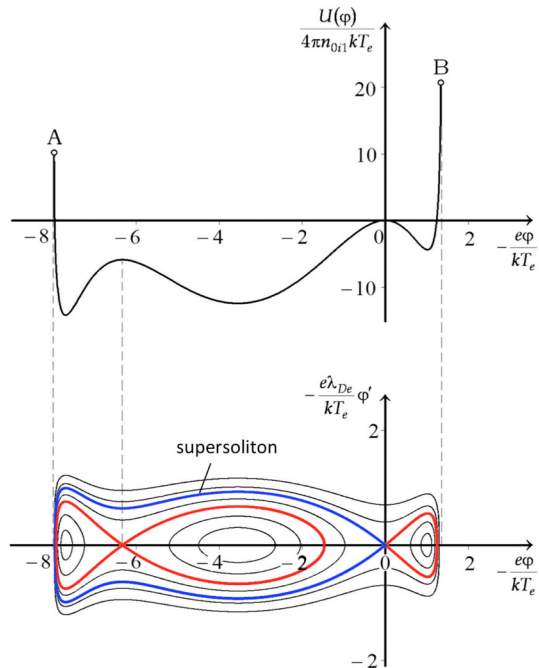
The dynamics of the cold and massive ion components in the ion-acoustic wave is governed by the set of hydrodynamic equations (3)–(4) and (15), while the hot and inertialess electrons and positrons are distributed in the wave according to the Boltzmann laws (2) and (16), respectively. Repeating the calculations performed in Eqs. (6)–(11), one can obtain a second-order ordinary differential equation with respect to the function $\varphi(\xi)$ where φ is an electrostatic potential in the wave, and $\xi \equiv x - Vt$ with V being a phase speed of the wave, which has a form of Eq. (12).

By definition, supersolitons are essentially large-amplitude structures; hence, for their analysis the perturbation theory approach based on the introduction of a small parameter into the model and reducing the initial set of equations to a single governing evolutionary equation of the Korteweg–de Vries (KdV) type are no longer applicable. Instead, supersolitary solutions determined by Eq. (12) can be successfully analysed with the use of the mechanical analogy approach, which uses the generalised potential energy function, also known as the *Sagdeev pseudopotential*, allowing for the studying of arbitrarily large-amplitude fluctuations. We recall, that according to the Sagdeev pseudopotential technique, Eq. (12) has a form of the equation of motion of a pseudoparticle, where φ and ξ play the role of the generalised coordinate and time, respectively, and the right-hand side of Eq. (12) can be treated as an effective force field governing the dynamics of a particle. Following this approach, Eq. (12) has an integral of motion written in the form of Eq. (13), with the Sagdeev pseudopotential function $U(\varphi)$ determined by Eq. (17).

The Sagdeev pseudopotential $U(\varphi)$ (17) allowing for the existence of supersolitons in *epii*-plasma and the corresponding phase portrait of the whole dynamical system (stationary ion-acoustic wave) are shown in Fig. 11. For certain values of the dimensionless parameters of the model, the function $U(\varphi)$ is found to have three local minima separated by two local maxima, with the most right maximum showing the so-called *saddle* point, where the initial equilibrium of an oscillating particle is unstable, and corresponding to the unperturbed state of the plasma. Such a configuration of the pseudopotential $U(\varphi)$ implies the existence of two separatrix layers in the phase portrait of the wave (see bottom plot of Fig. 11), with a certain separatrix enveloping the other in the region of negative values of the electrostatic potential φ , and thus corresponding to a supersolitary solution. We need to mention that Verheest (2009) also showed the Sagdeev pseudopotential of nonlinear dust-acoustic waves in a four-species *eidd*-plasma consisting of electrons, ions, and two dusty components of opposite electric charges, which could have three local minima and two maxima. However, in that example, the values of the dimensionless parameters of the model were adjusted to provide equal heights of the local maxima of the function $U(\varphi)$ (see Fig. 9 in Verheest 2009). The latter geometry of $U(\varphi)$ represents a limiting case, which supports the propagation of double layers in the plasma and prevents the existence of supersolitons. Hence, supersolitary solutions were not studied earlier by Verheest (2009).

Figure 12 allows one to compare stationary profiles of the electrostatic potential $\varphi(\xi)$ varying in a supersoliton (b) and in an ordinary soliton (a) of an ion-acoustic type in *epii*-plasma, obtained from numerical solutions of the governing Eq. (12).

Fig. 11 Sagdeev pseudopotential $U(\varphi)$ (17) (top) and the phase portrait (bottom) of an ion-acoustic wave in *epii*-plasma plotted for $n_{0i2}/n_{0i1} = 4.8$, $n_{0p}/n_{0i1} = 0.045$, $m_2/m_1 = 0.495$, $T_p/T_e = 1.02$, $\sqrt{m_1 V^2/kT_e} = 11.35$, $Z_1 = 48$, and $Z_2 = 4$. Separatrices of ordinary (KdV-like) solitons are shown by the red lines; a supersolitary separatrix is indicated by the blue line (adapted from Dubinov and Kolotkov 2012c)



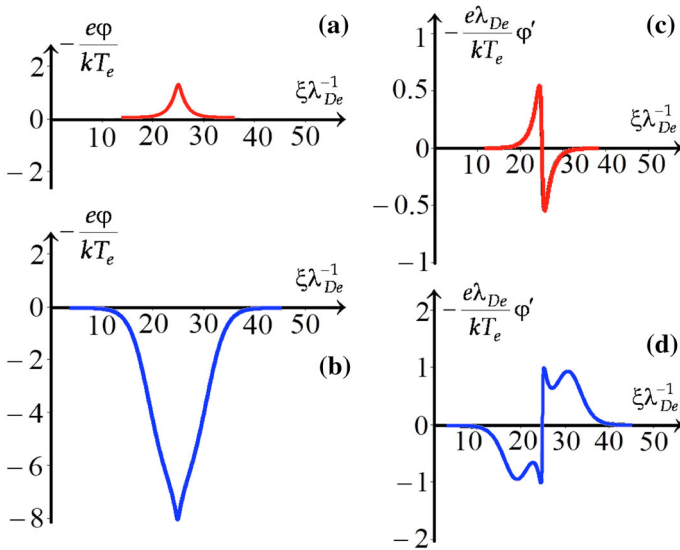


Fig. 12 Profiles of an ordinary ion-acoustic soliton (a) and supersoliton (b), propagating in *epii*-plasma and plotted for the same values of the dimensionless parameters of the model as shown in Fig. 11. Profiles of the first derivative of an ordinary ion-acoustic soliton (c) and supersoliton (d) in *epii*-plasma. Colours are consistent with those used in Fig. 11 (adapted from Dubinov and Kolotkov 2012c)

As supersolitons cannot be described by the KdV equation, their profiles highly differ from the ordinary bell-shaped soliton solutions determined by the $\text{sech}^2(x - Vt)$ function in a weakly nonlinear theory. In particular, variation of the electrostatic potential φ in the ion-acoustic supersolitary regime, shown in Fig. 12, has at least four points where its second derivative is zero. Additionally, amplitudes and widths of these supersolitary structures are always sufficiently larger compared to the ordinary KdV-solitons.

We would like to emphasise that electrostatic supersolitons exist in unmagnetised plasmas consisting of at least four electrically active components. Indeed, in simpler models of two- and three-species plasmas, the Sagdeev pseudopotential was empirically found to have up to two or three local extrema, respectively (see, e.g. Sect. 2.2). Hence, the required scenario when the external separatrix envelops the internal one cannot occur and supersolitons are impossible. There are a few additional conditions for the existence of supersolitons in a dynamical system, resulting from the analysis of the generalised potential energy function, $U(\varphi)$, namely the second maximum of the function $U(\varphi)$ must be always lower than its first maximum corresponding to the initial neutrality of the plasma (cf. Verheest 2009), while the point of the reflection of ions from the potential barrier in the wave (i.e. the point “A” in Fig. 11) must be always above it.

The contrast between super- and ordinary solitons becomes even more pronounced if one looks at the first derivative of the signal that can be used to distinguish them in laboratory experiments and astrophysical observations. In particular, Fig. 12 shows that the first derivative of the electrostatic potential φ , which is in fact the electric field magnitude, varying in the ordinary ion-acoustic

soliton (c) has only a single extremum on a half-period of the structure, while the supersolitary regime is characterised by the appearance of additional side extrema on the electric field profile (d). Moreover, the number of the equilibrium points in the phase portrait, enveloped by the corresponding separatrix, is unambiguously determined by the number of extrema in the first derivative of the supersoliton.

3.2 Supersolitons in a warm dusty *epiid*-plasma

In this section we demonstrate the possibility for the existence of ion-acoustic supersolitons in a more complicated multi-species plasma model, which accounts for the effect of a non-zero ion temperature and includes an additional negatively charged plasma component, for example static dusty grains. Similar to the previous section, the plasma is assumed to be uniform, collisionless, and unmagnetised. The initial full electrical neutrality condition for the unperturbed state of such a five-species plasma takes the form $Z_1en_{0i1} - Z_2en_{0i2} - en_{0e} + en_{0p} - q_d n_d = 0$, where an additional term $(-q_d n_d)$ describes the contribution of the dusty component, with $q_d < 0$ and n_d being its electric charge and concentration, respectively. The amount of the spatial electric charge of the dusty fraction relative to other plasma components is characterised by the dimensionless parameter $\alpha = q_d n_d / en_{0i1}$, which in turn allows one to rewrite the above neutrality condition as $n_{0e} = n_{0i1}(Z_1 - \gamma Z_2 + \delta - \alpha)$, where additional dimensionless parameters $\gamma = n_{0i2} / n_{0i1}$ and $\delta = n_{0p} / n_{0i1}$ are introduced.

The dynamics of the warm ion components in the wave is governed by the following set of hydrodynamic equations, which in contrast to the previous sections takes into account an additional restoring force produced by the ion thermal pressure gradients, $\partial P_{i1,2} / \partial x$:

$$\frac{\partial n_{i1,2}}{\partial t} + \frac{\partial(n_{i1,2} v_{i1,2})}{\partial x} = 0, \tag{40}$$

$$\frac{\partial v_{i1,2}}{\partial t} + v_{i1,2} \frac{\partial v_{i1,2}}{\partial x} = \pm \frac{Z_{1,2} e}{m_{i1,2}} \frac{\partial \varphi}{\partial x} - \frac{1}{m_{i1,2} n_{i1,2}} \frac{\partial P_{i1,2}}{\partial x}, \tag{41}$$

$$\frac{\partial^2 \varphi}{\partial x^2} = 4\pi e (Z_1 n_{i1} - Z_2 n_{i2} - n_e + n_p - \alpha n_{0i1}), \tag{42}$$

where in Eq. (41) the plus/minus sign refers to the positive/negative ions, respectively.

For simplicity, both ion components are assumed to be of the Maxwellian distribution in the wave, with the isothermal equations of state:

$$P_{i1,2} = n_{i1,2} k T_{i1,2}, \tag{43}$$

where the temperatures of different species are constant but in general different. The hot and inertialess electrons and positrons are still governed by the Boltzmann laws (2) and (16).

Introducing again the variable $\xi = x - Vt$ into set (40)–(43) and transforming it to a new frame of reference travelling with the phase speed of the wave, V as $u_{i1,2} = v_{i1,2} - V$, one can integrate the continuity equations (40) and the equations of motion (41) with the initial conditions $u_{i1,2} = -V$, $n_{i1,2} = n_{0i1,2}$, and $\varphi = 0$, and obtain explicit dependences of the ion concentrations $n_{i1,2}$ upon the electrostatic potential φ , as

$$\frac{n_{i1}(\varphi)}{n_{0i1}} = \left\{ -\frac{m_{i1}V^2}{kT_{i1}} \right\}^{1/2} \left\{ W_{0,-1} \left[-\frac{m_{i1}V^2}{kT_{i1}} \exp \left(-\frac{m_{i1}V^2}{kT_{i1}} - \frac{2Z_1e\varphi}{kT_{i1}} \right) \right] \right\}^{-1/2}, \quad (44)$$

$$\frac{n_{i2}(\varphi)}{n_{0i2}} = \left\{ -\frac{m_{i2}V^2}{kT_{i2}} \right\}^{1/2} \left\{ W_{0,-1} \left[-\frac{m_{i2}V^2}{kT_{i2}} \exp \left(-\frac{m_{i2}V^2}{kT_{i2}} + \frac{2Z_2e\varphi}{kT_{i2}} \right) \right] \right\}^{-1/2}, \quad (45)$$

with the Lambert W -function that has principal (main) “0” and lower “− 1” real branches (Corless et al. 1996; Valluri et al. 2000; Dubinova 2004; Dubinov and Dubinova 2005).

In fact, dependences (44) and (45) are of great importance in the discussed model, carrying the information about the ion momentum and ion number conservations in the wave. They are clearly seen to be multivalued functions, and those branches which do not correspond to the initial neutrality of the plasma should be disregarded. On the other hand, the branches passing through the plasma equilibrium point with the coordinates $n_{i1,2} = n_{0i1,2}$ and $\varphi = 0$ should be selected for further calculations. Analysis shows that in Eq. (44) the lower branch $W_{-1}(\dots)$ of the Lambert W -function should be taken for $m_{i1}V^2 > kT_{i1}$, while in the opposite case when $m_{i1}V^2 < kT_{i1}$ the principal branch $W_0(\dots)$ needs to be used. Similarly, in Eq. (45) one should choose the lower $W_{-1}(\dots)$ or principal $W_0(\dots)$ branch of the Lambert W -function, when $m_{i2}V^2 > kT_{i2}$ or $m_{i2}V^2 < kT_{i2}$, respectively.

Figure 13 shows dependences (44) and (45) plotted for the case when both lower branches $W_{-1}(\dots)$ satisfy the initial neutrality condition with $n_{i1,2} = n_{0i1,2}$ and $\varphi = 0$, while both principal branches $W_0(\dots)$ are physically meaningless and, hence, are disregarded. Furthermore, using coordinates of the conjugation point of the Lambert W -function real branches (we recall, that by its definition in the conjugation point the argument of the Lambert W -function is equal to $-\exp[-1]$), one can straightforwardly obtain the maximum and minimum values of the electrostatic potential φ , allowed in the wave (see Fig. 13):

$$\varphi_{\min} = -\frac{kT_{i2}}{2Z_2e} \left[\ln \left(\frac{m_{i2}V^2}{kT_{i2}} \right) - \frac{m_{i2}V^2}{kT_{i2}} + 1 \right], \quad (46)$$

$$\varphi_{\max} = \frac{kT_{i1}}{2Z_1e} \left[\ln \left(\frac{m_{i1}V^2}{kT_{i1}} \right) - \frac{m_{i1}V^2}{kT_{i1}} + 1 \right]. \quad (47)$$

Then substituting Eqs. (2), (16), (44), and (45) into Poisson’s law (42), one obtains the following second-order ordinary differential equation governing the dynamics of a stationary ion-acoustic wave in the warm dusty *epiid*-plasma:

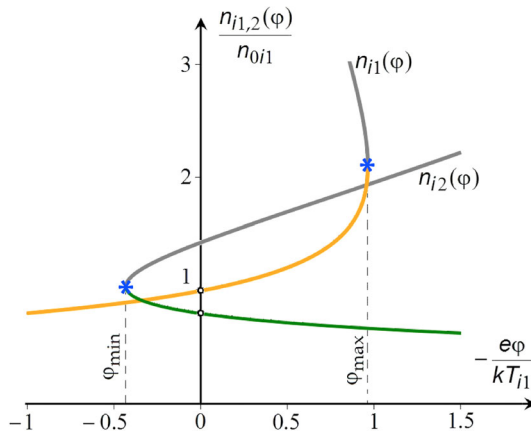


Fig. 13 Dependences (44) and (45) shown for $m_{i1}V^2 > kT_{i1}$ and $m_{i2}V^2 > kT_{i2}$, determined by the lower branch $W_{-1}(\dots)$ of the Lambert W -function (yellow and green lines, respectively). Blank circles correspond to the initial neutrality condition of the plasma, $n_{i1,2} = n_{0i1,2}$ and $\varphi = 0$. Grey lines show the principal branch $W_0(\dots)$ of the Lambert W -function in dependences (44) and (45), not corresponding to the initial neutrality of the plasma. Blue asterisks show the conjugation points of real branches of dependences (44) and (45), determined by the Lambert W -function (adapted from Dubinov and Kolotkov 2012b)

$$\frac{d^2\varphi}{d\xi^2} = 4\pi\rho(\varphi), \tag{48}$$

where

$$\begin{aligned} \rho(\varphi) = & Z_1en_{0i1} \left\{ -\frac{kT_{i1}}{m_{i1}V^2} W_{0,-1} \left[-\frac{m_{i1}V^2}{kT_{i1}} \times \exp \left(-\frac{m_{i1}V^2}{kT_{i1}} - \frac{2Z_1e\varphi}{kT_{i1}} \right) \right] \right\}^{-1/2} \\ & - Z_2en_{0i2} \left\{ -\frac{kT_{i2}}{m_{i2}V^2} W_{0,-1} \left[-\frac{m_{i2}V^2}{kT_{i2}} \exp \left(-\frac{m_{i2}V^2}{kT_{i2}} + \frac{2Z_2e\varphi}{kT_{i2}} \right) \right] \right\}^{-1/2} \\ & - n_{0e}e \exp \left(-\frac{e\varphi}{kT_e} \right) + n_{0p}e \exp \left(\frac{e\varphi}{kT_p} \right) - \alpha en_{0i1}. \end{aligned}$$

Following the mechanical analogy formalism, Eq. (48) has the Sagdeev pseudopotential, $U(\varphi) = -4\pi \int_0^\varphi \rho(\varphi) d\varphi$ written in the explicit form as

$$\begin{aligned} \frac{U(\varphi)}{4\pi kT_{i1}} = & n_{0i1} \left[\mathcal{R}_1(\zeta_{01}) - \mathcal{R}_1(\zeta_1) \right] + n_{0i2} \left[\mathcal{R}_2(\zeta_{02}) - \mathcal{R}_2(\zeta_2) \right] \\ & + n_{0e} \frac{T_e}{T_{i1}} \left[1 - \exp \left(-\frac{e\varphi}{kT_e} \right) \right] + n_{0p} \frac{T_p}{T_{i1}} \left[1 - \exp \left(\frac{e\varphi}{kT_p} \right) \right] + \alpha n_{0i1} \frac{e\varphi}{kT_{i1}}, \end{aligned} \tag{49}$$

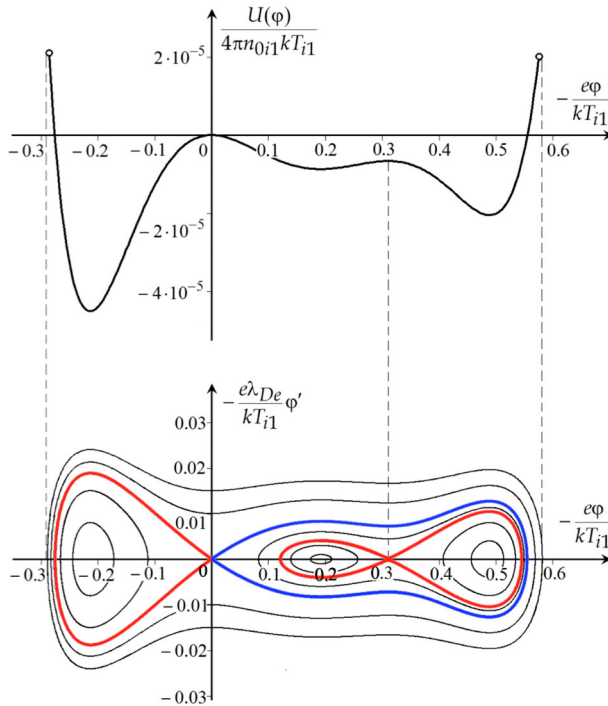


Fig. 14 Pseudopotential $U(\varphi)$ (49) (top) and the phase portrait (bottom) of an ion-acoustic wave in a warm dusty *epiid*-plasma plotted for $\alpha = 0.1852$, $\gamma = 0.8$, $\delta = 0.13$, $T_p/T_e = 0.87$, $T_{i1}/T_e = 1.76$, $T_{i2}/T_e = 9.2$, $\sqrt{m_{i1}V^2/kT_e} = 2.1$, $m_{i2}/m_{i1} = 2$, and $Z_1 = Z_2 = 1$. Blank circles correspond to the reflection of ions from the potential barrier in the wave. λ_{De} is the electron plasma Debye length. The colour scheme is identical to that used in Fig. 11 (adapted from Dubinov and Kolotkov 2012b)

where

$$\zeta_{1,2} = -\frac{m_{i1,2}V^2}{kT_{i1,2}} \mp \frac{2Z_{1,2}e\varphi}{kT_{i1,2}}, \quad \zeta_{01,2} \equiv \zeta_{1,2}(\varphi = 0), \quad \text{and}$$

$$\mathcal{R}_{1,2}(\zeta_{1,2}) = \frac{(T_{i1,2}/T_{i1}) W_{-1}[\zeta_{01,2} \exp(\zeta_{1,2})] + 1}{\{\zeta_{01,2} W_{-1}[\zeta_{01,2} \exp(\zeta_{1,2})]\}^{1/2}}.$$

Figure 14 shows the Sagdeev pseudopotential $U(\varphi)$ determined by Eq. (49) and the corresponding phase portrait of nonlinear stationary ion-acoustic waves propagating in the warm dusty *epiid*-plasma plotted for certain values of the dimensionless parameters of the model. Similar to previous Sect. 3.1, the geometry of the generalised potential energy $U(\varphi)$ is clearly seen to correspond to the existence of supersolitary solutions in the discussed five-species plasma model, i.e. there are three local minima in the potential energy function $U(\varphi)$ and there is an external separatrix, which fully envelops the internal one, in the phase portrait. For comparison, Fig. 15 illustrates variations of the normalised electrostatic potential φ and its first derivative (that is an effective electric field in the wave) in the ordinary

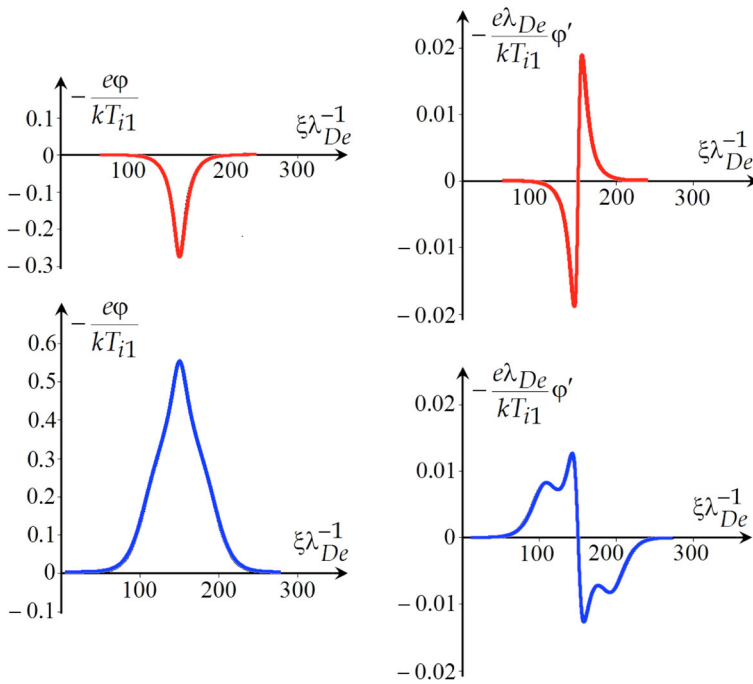


Fig. 15 Profiles of an ordinary ion-acoustic soliton (top left) and supersoliton (bottom left) propagating in a warm dusty *epiid*-plasma. Profiles of the first derivative of an ordinary ion-acoustic soliton (top right) and supersoliton (bottom right) in a warm dusty *epiid*-plasma. Colours are consistent with those used in Fig. 14 (adapted from Dubinov and Kolotkov 2012b)

and supersolitary regimes obtained from numerical solutions of the governing equation (48).

3.3 Further development of the concept of supersolitons in plasma

The idea of supersolitons, originally proposed by Dubinov and Kolotkov (2012a, b, c), has opened a new actively developing research area in the field of nonlinear waves in plasma. Since the discovery of this type of waves in plasma in 2012, tens of follow-up and original studies were published, indicating the possibility of their existence in various plasma models and analysing their physical properties. The Sagdeev pseudopotential technique was used in all these works as a conventional instrument for analysis. In this paragraph we briefly outline state-of-the-art achievements obtained in the theory of supersolitons in plasma during these 5 years.

Verheest et al. (2013) shows that electrostatic supersolitons are not a feature of exotic, complicated plasma models, but can exist even in a three-species non-thermal plasma and are likely to occur in space plasmas. A methodology is given to derive their existence domains in a systematic manner by determining the specific limiting factors. A model of plasma with two groups of kappa-distributed electrons

is considered in Verheest et al. (2013), where the ion-acoustic supersolitons are shown to exist too. Properties of ion-acoustic supersolitons in a plasma with two-temperature electrons, positrons, and ions (treating all the light plasma components as non-thermal) are studied in Dutta et al. (2014). Steffy and Ghosh (2017) explore a transition of an ordinary ion-acoustic soliton into a supersoliton in a four-species plasma with two groups of electrons and two sorts of ions, delineating the parametric ranges of the existence of supersolitons. Ion-acoustic solitary waves with a W-shaped profile are found in a four-component plasma in Paul et al. (2016). Such type of solitons may be also referred to as supersolitons.

A series of publications, Rufai et al. (2014, 2015, 2016a, b) and Rufai (2015), investigate the details of oblique (with respect to the magnetic field) propagation of ion-acoustic supersolitons in a magnetised auroral plasma. Ion-beam plasmas with stationary dust grains are also found to support ion-acoustic supersolitons (Dutta and Sahu 2017). It turns out that not only ion-acoustic waves in multi-component plasmas can have a form of supersolitons. For example, a possibility for the existence of dust-acoustic supersolitons in a four-component dusty plasma is shown in El-Wakil et al. (2017).

An important step forward in the theory of supersolitons in plasma has been made by Olivier et al. (2017), where the mathematical formalism based on the Taylor expansion of the Sagdeev pseudopotential $U(\varphi, M)$ in the vicinity of the acoustic speed M and the equilibrium electrostatic potential φ is developed for a description of low-amplitude supersolitons in a general fluid model consisting of an arbitrary number of species. The authors derive a simplified form of the Sagdeev pseudopotential as a fifth-order polynomial (cf. Eqs. 17 and 49), which is able to support supersolitons

$$U(\varphi, M) = A\delta M\varphi^2 + B\varphi^3 + C\varphi^4 + D\varphi^5, \quad (50)$$

where δM is the incremental velocity and the constant coefficients A , B , C , and D are always non-zero and determined by the equilibrium parameters of the plasma.

3.4 Minimum number of plasma species needed for the existence of electrostatic supersolitons

Section 3.1 and Dubinov and Kolotkov (2012c) conclude with an important fact that parallel electrostatic supersolitons can exist in plasmas with at least four electrically charged components. For example, it was previously found that for simpler two- and three-species plasma models the Sagdeev pseudopotential can have up to two or three local extrema, respectively (see, e.g. Sect. 2.2). In these cases, it is impossible for the external separatrix to envelop the internal one, and thus a supersoliton cannot exist. This simple empirical rule has been recently independently confirmed by Verheest et al. (2014), where the authors rigorously proved the absence of electrostatic supersolitons in two-species plasmas. On the other hand, in the work by Verheest et al. (2013) a three-species *eei*-plasma model supporting supersolitary solutions was developed, thus contradicting the above conclusions. However, the latter discrepancy can be easily resolved by a closer view at the electron distribution

functions used in the models. More specifically, in Dubinov and Kolotkov (2012b, c) and Dubinov et al. (2012a) light and hot particles were assumed to be distributed by the Boltzmann law having the form of Eq. (2), which cannot be separated into individual energetic groups. In contrast, Verheest et al. (2013, 2014) used the following non-thermal distribution function for the electron plasma component (given in the normalised form),

$$n_e(\varphi) = (1 - \beta\varphi + \beta\varphi^2) \exp(\varphi), \quad (51)$$

where φ is the normalised electrostatic potential in the wave, and β is the parameter of the electron non-thermality. Distribution (51) reduces to the traditional Boltzmann distribution (2) only in the limiting case $\beta = 0$, i.e. when all the non-thermal effects are suppressed, while for $\beta \neq 0$ it describes the evolution of three separate electron populations (one thermal and two non-thermal). Essentially, each separate electron in the plasma is able to contribute to only a single population among those three on the right-hand side of Eq. (51), which in turn appear as three individual terms in Poisson's equation. For example, if one considers a plasma consisting of the electrons distributed by Eq. (51) and ions, it could be treated as a two-species plasma according to the formulation used in Verheest et al. (2013). On the other hand, it is in fact a four-species plasma, as there are four terms (corresponding to one ion and three electron populations) on the right-hand side of Poisson's equation. Moreover, this formulation is also applicable to an example of dust-acoustic waves in a plasma with non-thermal positively charged ionic components distributed by

$$n_i(\varphi) = (1 + \beta\varphi + \beta\varphi^2) \exp(-\varphi), \quad (52)$$

which was considered by Mendoza-Briceño et al. (2000) in the application to space and astrophysical dusty plasma situations.

Another illustrative example is given by Rufai et al. (2015), where the analytical model of the magnetised plasma consisting of a cold ion fluid and cool Boltzmann and hot kappa-distributed electrons was developed. Again according to Verheest et al. (2013), it represents a two-species plasma, where the obliquely propagating ion-acoustic supersolitons were successfully detected (cf. Verheest et al. 2014). Hence, the correct accounting of the light component populations, included in the multi-species plasma model, is essential when analysing the possibility for the existence of supersolitary solutions. We would like to finalise the current discussion pointing out that unjustified partitioning of plasma electrons into several species of different energies sometimes may lead to erroneous results (Yu and Luo 2008).

4 Periodic SNW and supersolitons in space, laboratory, and numerical experiments

4.1 Signatures of SNW and supersolitons detected in earlier records

Nonlinear oscillatory phenomena in astrophysical and laboratory plasmas are regularly observed with the imaging and spectral instruments throughout the whole

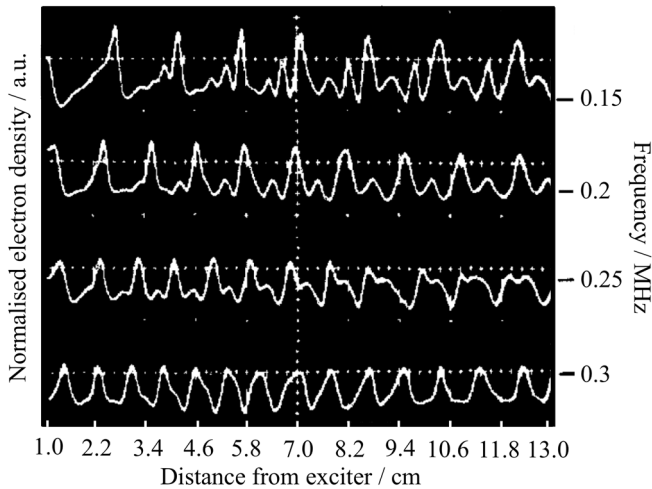


Fig. 16 Variations of the electron density in the propagating ion-acoustic wave excited at various frequencies in a large double-plasma device (adapted from Ikezi 1973)

electromagnetic spectrum. More specifically, electrostatic waves in plasma are usually measured in experiments as the variations of electrostatic potential or concentration of a certain plasma component. Also, the time variability of a local electric field recorded at the location of a measuring detector is often of interest in plasma experiments. According to the theory developed above, a physical quantity experiencing oscillations in a periodic SNW or supersoliton would have an oscillation profile with characteristic wiggles (see, e.g. Figs. 4, 7, 10, and the bottom left panels in Figs. 12 and 15) and non-monotonic patterns (see, e.g. the bottom right panels in Figs. 12 and 15), which enable the discussed waves to be identified in experimental records. The latter behaviour is determined by a number of separatrices enveloped by a phase trajectory of the wave (see Sect. 2.1). A comprehensive literature survey shows that there are a great number of earlier works reporting on the experimental detection of periodic and solitary waves in laboratory plasma machines and space missions, which have very straightforward signatures of SNW and supersolitons. However, the presence of those wiggling and non-monotonic patterns in the observational signals was usually ignored by the authors. In this section we summarise several most illustrative observational examples obtained in space, laboratory and numerical plasma experiments, which can be considered as potential candidates for SNW and supersolitons.

Ikezi (1973) shows profiles of periodic ion-acoustic waves excited at various frequencies in a large double-plasma device (Taylor et al. 1972). Behaviour of the electron concentration in the observed propagating wave is reproduced in Fig. 16. These wiggling and non-monotonic profiles are clearly different from a cnoidal form of usual nonlinear ion-acoustic waves in a two-component electron-ion plasma (Dubinov 2007) and may be possibly referred to as one of the earliest observational evidences of periodic ion-acoustic SNW.

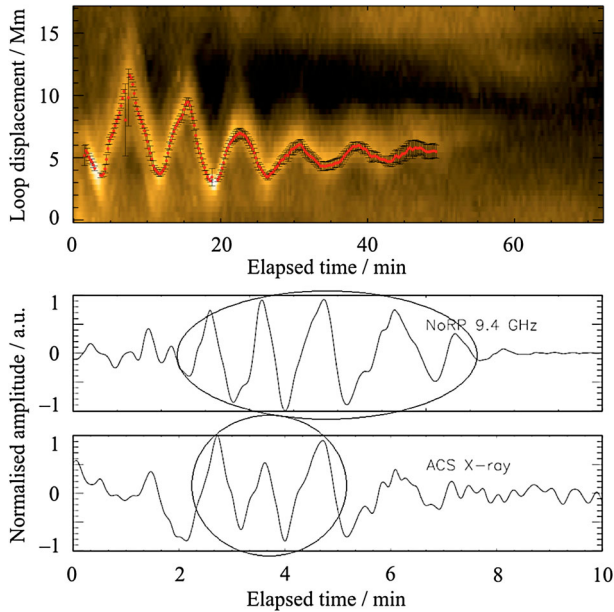


Fig. 17 Time–distance map showing an anharmonic profile of a standing fast magnetoacoustic mode of a coronal loop, detected with the Atmospheric Imaging Assembly on-board the Solar Dynamics Observatory mission, in the extreme ultraviolet band. The elapsed time starts at 20:41:48.34 UT, 26 May 2012 (top, adapted from Pasco et al. 2016). Anharmonic quasi-periodic pulsations of a symmetric triangular shape in an X1.2 class solar flare on 29 May 2003, observed in the radio band at 9.4 GHz with the Nobeyama Radio Polarimeters (middle) and in the hard X-ray band (bottom), measured with the ACS instrument on-board the INTEGRAL satellite. The elapsed time starts at 01:00 UT (adapted from Nakariakov et al. 2010)

More recent examples clearly illustrating typical signatures of periodic SNW were detected in the magnetised plasma of the solar atmosphere, a natural laboratory for studying fundamental plasma processes including nonlinear waves and oscillations (Nakariakov and Verwichte 2005; Nakariakov et al. 2016). In particular, Nakariakov et al. (2010) detected so-called quasi-periodic pulsations (QPP) in the electromagnetic emission of a powerful X1.2 class solar flare which occurred on 29 May 2003. The oscillations were found in two independent observations made with the Nobeyama Radio Polarimeters and with the ACS instrument on-board the INTEGRAL satellite in the radio and hard X-ray band, respectively. Spectral analysis of the observational signals, performed with the use of the empirical mode decomposition technique (EMD), revealed that the oscillations shown in the bottom panels of Fig. 17 have an anharmonic profile of a symmetric triangular shape with several points on a single oscillation cycle, where its second derivative equals zero, which are typical signatures of the discussed SNWs. Furthermore, the following temporal evolution of the oscillation profile shows a well-pronounced rapid decrease of the oscillation amplitude, which may look similar to the transformation of the wave type from SNW to NW through a


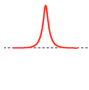
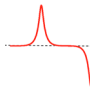
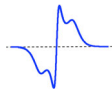


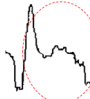

separatrix, as proposed in Sect. 2.1. Similar anharmonic and non-stationary QPPs are often seen in other flaring events and most likely require involvement of the discussed higher order nonlinear effects for the interpretation (see, e.g. Nakariakov and Melnikov 2009; Van Doorselaere et al. 2016, for recent reviews).

A standing fast magnetoacoustic mode of a coronal loop can also manifest typical SNW signatures (Pasco et al. 2016), as shown in the top panel of Fig. 17. The oscillation profile was obtained from a high-resolution time–distance map created with the Atmospheric Imaging Assembly on-board the Solar Dynamics Observatory, AIA/SDO in the extreme ultraviolet band. Before the loop displacement gets sufficiently damped, the first few oscillation cycles clearly represent highly anharmonic behaviour with a symmetric triangular shape and well-distinguished wiggles.

In addition to typical signatures of periodic SNW, space plasma observations often show intensive bursts of the electric field, occurring in the form of electrostatic supersolitons. For example, the space missions S3-3 (6000–8000 km, Temerin et al. 1982), Viking (817–13,527 km, Bostrom et al. 1988), Polar (up to 10,000 km, Mozer et al. 1997), and FAST (350–4175 km, Ergun et al. 1998) were used for registration of electrostatic solitary structures in the magnetospheric plasma, such as ion-acoustic solitons, double layers, and phase holes. Their records are widely available in the literature and often contain certain patterns which can be interpreted as supersolitons. The difference between the electric field profiles in an ordinary (KdV-type) ion-acoustic soliton, ion double layer, ion phase hole, and ion-acoustic supersoliton is illustrated in Table 1. More specifically, parallel component of the electric field in a conventional ion-acoustic soliton/ion double layer has a localised symmetric bipolar/unipolar structure, respectively; in an ion phase hole it is always constrained by two double layers of opposite polarities; while the electric field profile associated with an ion-acoustic supersoliton is inherently different from that in traditional solitary structures, having additional extrema on the wings. The latter can be used for distinguishing of these localised electrostatic ion structures and detection of supersolitons in observations. For example, Fig. 18 shows potential candidates for electrostatic supersolitons detected in the Earth's auroral plasma and chosen on the basis of the unique properties given in Table 1. The top panel of Fig. 18 illustrates a single bidirectional structure of the electric field, observed near Southern auroral oval simultaneously by three out of four Cluster satellites, on 23 January 2001 (Gustafsson et al. 2001). The structure is clearly seen to be embroidered with subsidiary local extrema (wiggles) on its both wings, coinciding with the expected behaviour of the electric field in electrostatic supersolitons. The bottom panel of Fig. 18 shows a 20 ms portion of observations of a parallel electric field measured in the high-altitude polar magnetosphere by the polar plasma wave instrument (PWI) on 4 June 1997 (Franz et al. 2005). Although the authors were searching for phase holes in the observational data, at least two distinct pulses (delineated in Fig. 18) behave rather like supersolitons than phase holes or ordinary solitary waves (cf. Table 1).

Consider another type of experiments, numerical simulations, where possible candidates for supersolitary solutions were detected too. Earlier works (Lu et al. 2005; Kakad et al. 2014) show 1D electrostatic particle-in-cell simulations of

Table 1 Expected theoretical profiles of the parallel electric field in an ordinary (KdV-type) ion-acoustic soliton, ion double layer, ion phase hole, and ion-acoustic supersoliton and their experimental analogies with corresponding references

Localised electrostatic ion structures	Ion-acoustic soliton	Ion double layer	Ion phase hole	Ion-acoustic supersoliton
Theoretical profiles of E_z				
Recorded profiles of E_z				
References	Fragment of Fig. 3 (Bostrom et al. 1988)	Fragment of Fig. 1p (Vasko et al. 2015)	Fragment of Fig. 7 (Goldman et al. 1999)	Fragment of Fig. 7b (Lu et al. 2005)

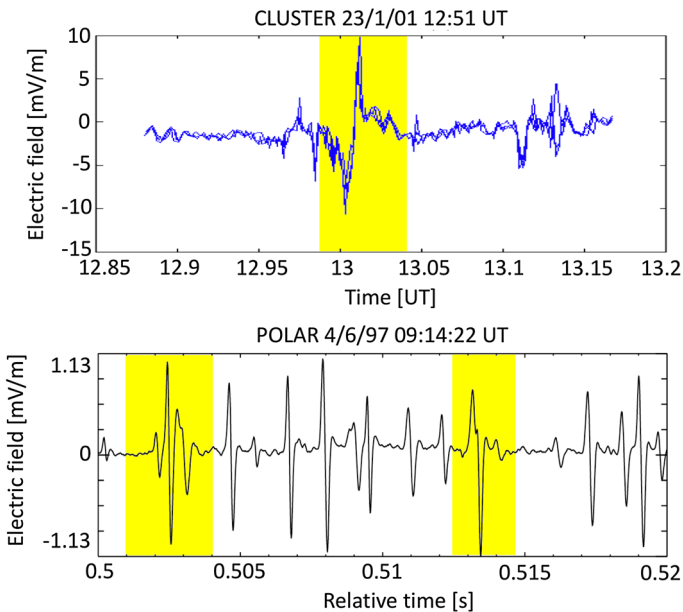


Fig. 18 Possible candidates for supersolitons (highlighted by yellow) detected in the high-altitude Earth’s auroral plasma. Top: a coherent solitary bidirectional electric field structure observed by the cluster electric field and wave (EFW) instrument. The time is given in hours and decimal of hours (adapted from Gustafsson et al. 2001). Bottom: 20 ms measurements of the parallel electric field observed by the Polar Plasma Wave Instrument (PWI) in the high-altitude polar magnetosphere (adapted from Franz et al. 2005)

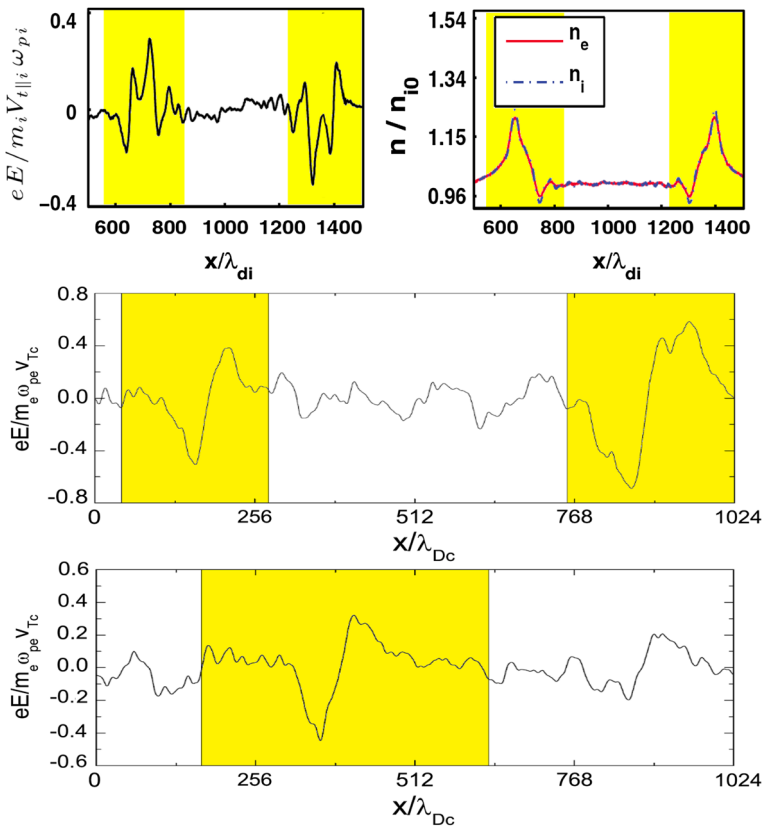


Fig. 19 Possible candidates for supersolitons (highlighted by yellow) detected in earlier particle-in-cell simulations of electrostatic solitary structures in the Earth's magnetospheric plasma. Top panels: spatial distribution of the electron and ion concentrations (right) and electric field (left) simulated in an electron–ion plasma perturbed by a Gaussian pulse (adapted from Kakad et al. 2014). Middle and bottom panels: spatial profiles of electrostatic field detected in a three-component plasma excited by the electron beam. The profiles were obtained in two numerical realisations with different equilibrium parameters of the plasma (adapted from Lu et al. 2005)

nonlinear evolution of electrostatic solitary waves in space plasmas, particularly focusing on the Earth's auroral regions. The electric fields detected in simulations are shown in Fig. 19 and have a localised bipolar structure with well-distinguished non-monotonic patterns and wiggles, which is consistent with the form of electrostatic supersolitons predicted by theory (see Table 1).

Kakad et al. (2016) shows 1D modelling of the dynamics of a Gaussian perturbation of plasma density in a three-species plasma with cold ions and two groups of kappa-distributed electrons, performed within the hydrodynamic numerical scheme developed by Lotekar et al. (2016). The initial perturbation was found to rapidly transform into an ion-acoustic supersoliton propagating further with a distinctly wiggling shape and constant speed. The results of these simulations obtained at two different instants of the computational time are illustrated

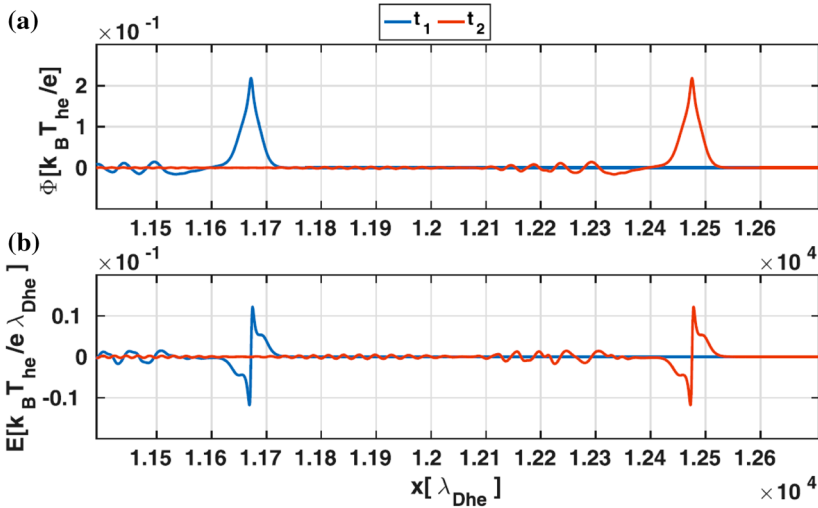


Fig. 20 First dedicated numerical modelling of the ion-acoustic supersoliton in plasma, formed from the initial density perturbation of a Gaussian shape. Top and bottom panels show the behaviour of the electrostatic potential (a) and electric field (b) in the observed supersoliton. Red and blue curves are obtained at two different instants of the computational time (taken from Kakad et al. 2016)

in Fig. 20. We would like to emphasise the importance of this work, which is in fact the first-ever dedicated numerical simulation of ion-acoustic supersolitons in plasma.

The question of the detection of supersolitons in laboratory experiments with chemically active plasmas is addressed in detail in Sect. 4.2 and references therein.

4.2 Supersolitons detected in laboratory experiments with SF₆-Ar-plasma with negative ions

Ion-acoustic solitary structures have been actively studied in laboratory experiments with a chemically active plasma representing a mixture of the ionised sulphur hexafluoride, SF₆ and argon, Ar gases (see, e.g. Nakamura 1982; Ludwig et al. 1984; Nakamura et al. 1985; Nakamura and Tsukabayashi 1985; Cooney et al. 1991a, b, and references therein). In addition to the electron population and tiny fractions of other components, the positive Ar⁺, SF₅⁺ and negative F⁻, SF₅⁻ ions are believed to be the most abundant species in such a plasma (according to Ludwig et al. 1984). The interest in these experiments has been stimulated by a number of in situ and remote observations reporting an important role of negative ions in the processes operating in the lower ionosphere and atmosphere, such as nightglows (see, e.g. detailed studies Swider et al. 1988, 1992) and ball lightnings (see, e.g. Smirnov 1993, for a comprehensive review). Additionally, the presence of negatively charged dusty grains can strongly affect physical processes, for example, in the plasma of cometary comas, planetary ring systems, accretion discs, and the transient atmospheres near the Moon and Mercury surfaces (see, e.g. Popel and

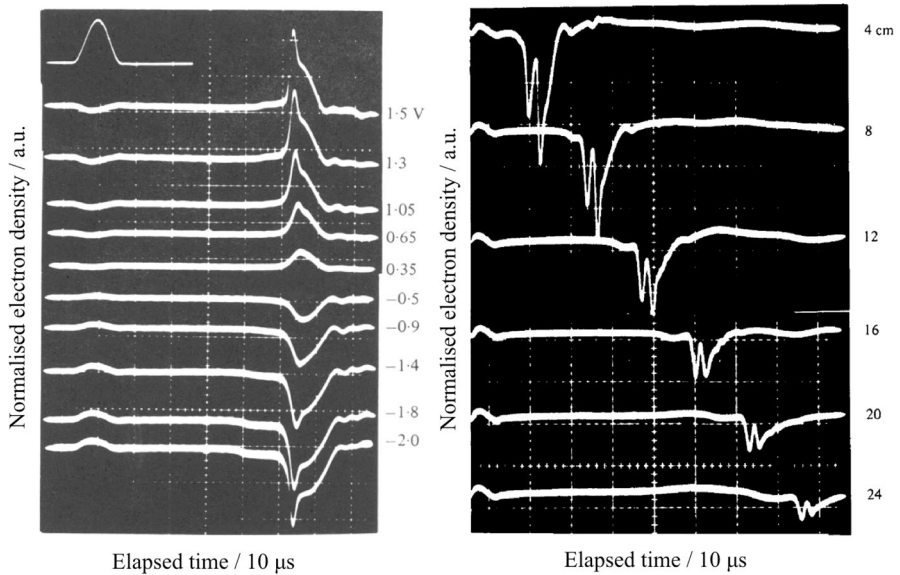


Fig. 21 Left: oscilloscope traces showing relative variations of the electron concentration in the ion-acoustic solitons propagating through SF₆-Ar-plasma. Different curves correspond to different amplitudes of the initial excitation, which are given on the right-hand side. Profile of the initial excitation is illustrated in the top left corner. Three top and three bottom curves have a clear anharmonic (wiggling) shape, typical for supersolitons (adapted from Nakamura and Tsukabayashi 1985). Right: oscilloscope traces showing the electron concentration in the ion-acoustic rarefaction solitons in SF₆-Ar-plasma, measured at different distances (shown on the right-hand side) from the initial excitation site. All curves clearly show a non-monotonic behaviour with a few extrema (adapted from Nakamura et al. 1985)

Gisko 2006, and references therein). Other interesting phenomena (such as formations of ion-acoustic shocks, discontinuities, and negative ion density fronts) appearing in plasmas with negative ions are described in Kaganovich and Tsendin (1993), Takeuchi et al. (1998), and Kaganovich et al. (2000). In almost all the laboratory experiments described in the above publications, large-amplitude ion-acoustic solitons of unusual form were detected. More specifically, they were found to be highly different from a traditional bell-shaped KdV-soliton, with a distinctly wiggling profile containing a few points where its second derivative equals zero. In some cases, the solitary structures were recorded to have non-monotonic slopes with a few clearly distinguished extrema. Examples of these “unusual” and “non-monotonic” ion-acoustic solitons observed in SF₆-Ar-plasma are illustrated in Fig. 21. Interestingly, these observational facts are inconsistent with previous analytical theories dealing with solitary waves in plasma systems, and these anomalies were not addressed in the studies listed above. On the other hand, these detected unusual properties (wiggling and non-monotonic profiles) of the ion-acoustic solitary structures shown in Fig. 21 are clearly seen to be similar to the typical signatures of supersolitons and their first derivatives (see, e.g. Figs. 12 and 15). In this section, the concept of supersolitons is employed for the interpretation of these unusual forms of ion-acoustic solitons shown in Fig. 21, and a theoretical

possibility for the existence of supersolitary solutions in a chemically active SF₆-Ar-plasma is demonstrated.

Consider a uniform, collisionless, and unmagnetised multi-species plasma consisting of the singly-charged positive Ar⁺, SF₅⁺ and negative F⁻, SF₅⁻ ions, and electrons. The initial neutrality condition for the equilibrium state of such a plasma has a form $en_{0Ar^+} - en_{0F^-} + en_{0SF_5^+} - en_{0SF_5^-} - en_{0e} = 0$, where $e < 0$ is the electric charge of the electron and negative ion components, $(-e) > 0$ is the electric charge of the positive ions, and the subscript “0” hereafter refers to the unperturbed values of the plasma parameters. Introducing the dimensionless parameters of the model, $\alpha = n_{0F^-}/n_{0Ar^+}$, $\beta = n_{0SF_5^-}/n_{0Ar^+}$, and $\gamma = n_{0SF_5^+}/n_{0Ar^+}$, the above neutrality condition can be rewritten as $n_{0e} = n_{0Ar^+}(1 - \alpha - \beta + \gamma)$. Absolute values of these parameters can be estimated from the actual experimental conditions used in Ludwig et al. (1984), where the partial pressure of the primary SF₆ molecular gas in the discharge chamber was taken to be low, hence $n_{0SF_6} \ll n_{0e}$. In this case, under a constant discharge current the initial concentration of the F⁻ ion gas is naturally lower than that of the SF₅⁻ ion gas, resulting to $\alpha \ll \beta$. Moreover, Ludwig et al. (1984) established additional empirical relations for the relative concentrations of the ion components in the performed experiment: $0.65 < n_{0SF_5^-}/(n_{0SF_5^-} + n_{0F^-}) < 0.95$ and $0.11 < n_{0SF_5^+}/(n_{0SF_5^+} + n_{0Ar^+}) < 0.77$, allowing one to obtain that $0.027 < \alpha < 0.28$ and $0.12 < \gamma < 3.35$ for a certain value of $\beta = 0.52$. Hence, the following values of the parameters $\alpha = 0.035$, $\beta = 0.52$, and $\gamma = 0.2$ were chosen for further analysis.

In the model, the electrons are assumed to be inertialess and hot with a constant temperature, and are, therefore, distributed by the Boltzmann law (2) in the wave. The massive ion gases are taken to be of a sufficiently low temperature allowing for the neglecting of the effect of the ion thermal pressure on the ion wave dynamics, which is governed by the following set of hydrodynamic equations:

$$\frac{\partial n_l}{\partial t} + \frac{\partial(n_l v_l)}{\partial x} = 0, \tag{53}$$

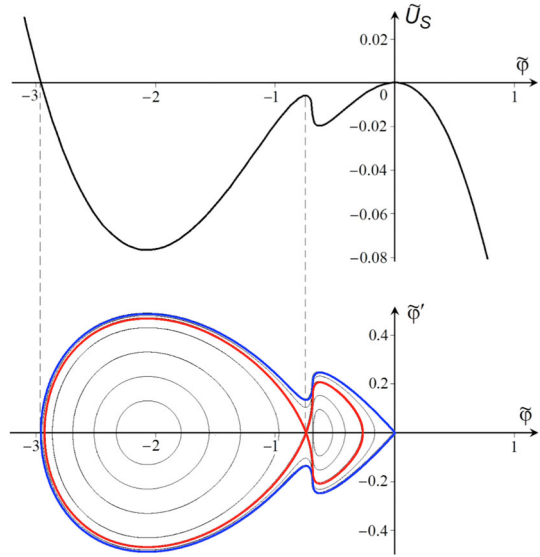
$$\frac{\partial v_l}{\partial t} + v_l \frac{\partial v_l}{\partial x} = \pm \frac{e}{m_l} \frac{\partial \varphi}{\partial x}, \tag{54}$$

$$\frac{\partial^2 \varphi}{\partial x^2} = 4\pi e(n_{Ar^+} - n_{F^-} + n_{SF_5^+} - n_{SF_5^-} - n_e), \tag{55}$$

where $l = Ar^+, F^-, SF_5^+, SF_5^-$, and the plus/minus sign in the equation of motion (54) refers to the positive/negative ions, respectively.

Similar to the previous models, one can introduce the variable $\xi = x - Vt$ into the set (53)–(55), transfer it to a new frame of reference, travelling with the phase speed of the wave, V , and afterwards derive the Sagdeev pseudopotential $U_S(\varphi)$ of the whole dynamical system, depending upon the electrostatic potential φ in the wave, as

Fig. 22 Dependence of the Sagdeev pseudopotential $U_S(\varphi)$ (56) (top) upon the electrostatic potential φ , and the phase portrait (bottom) of an ion-acoustic wave in SF₆-Ar-plasma, normalised as following: $\tilde{U}_S = U_S/4\pi n_{0Ar^+} kT_e$, $\tilde{\varphi} = -e\varphi/kT_e$, $\tilde{\varphi}' = -e\lambda_{De}(kT_e)^{-1}(d\varphi/d\xi)$, where λ_{De} is the electron plasma Debye length. The colour scheme is identical to that used in Fig. 11 (adapted from Dubinov et al. 2012a)



$$\begin{aligned}
 U_S(\varphi) = -4\pi \int_0^\varphi \rho(\varphi) d\varphi = 4\pi m_{Ar^+} V^2 \left\{ n_{0Ar^+} \left[1 - \left(1 + \frac{2e\varphi}{m_{Ar^+} V^2} \right)^{1/2} \right] \right. \\
 + n_{0F^-} \frac{m_{F^-}}{m_{Ar^+}} \left[1 - \left(1 - \frac{2e\varphi}{m_{F^-} V^2} \right)^{1/2} \right] + n_{0SF_5^-} \frac{m_{SF_5^-}}{m_{Ar^+}} \left[1 - \left(1 - \frac{2e\varphi}{m_{SF_5^-} V^2} \right)^{1/2} \right] \\
 \left. + n_{0SF_5^+} \frac{m_{SF_5^+}}{m_{Ar^+}} \left[1 - \left(1 + \frac{2e\varphi}{m_{SF_5^+} V^2} \right)^{1/2} \right] + n_{0e} \frac{kT_e}{m_{Ar^+} V^2} \left[1 - \exp\left(-\frac{e\varphi}{kT_e} \right) \right] \right\}, \tag{56}
 \end{aligned}$$

where

$$\begin{aligned}
 \rho(\varphi) = en_{0Ar^+} \left(1 + \frac{2e\varphi}{m_{Ar^+} V^2} \right)^{-1/2} - en_{0F^-} \left(1 - \frac{e\varphi}{m_{F^-} V^2} \right)^{-1/2} \\
 - en_{0SF_5^-} \left(1 - \frac{e\varphi}{m_{SF_5^-} V^2} \right)^{-1/2} + en_{0SF_5^+} \left(1 + \frac{e\varphi}{m_{SF_5^+} V^2} \right)^{-1/2} - en_{0e} \exp\left(-\frac{e\varphi}{kT_e} \right).
 \end{aligned}$$

Figure 22 shows the pseudopotential $U_S(\varphi)$ determined by Eq. (56) of an oscillating pseudoparticle, i.e. of the stationary ion-acoustic wave, and the corresponding phase portrait of the whole dynamical system plotted for $\sqrt{m_{Ar^+} V^2/kT_e} = 1.7$, that provides the phase speed of the wave, V to be certainly supersonic, and for $m_{SF_5^+}/m_{Ar^+} = 3.18$, $m_{SF_5^-}/m_{Ar^+} = 3.18$, and $m_{F^-}/m_{Ar^+} = 0.476$. This analysis indicates that indeed a large-amplitude supersolitary solution is possible in the developed SF₆-Ar-plasma model, whose phase trajectory, the external separatrix in the phase portrait, is of a guitar-like form and envelops the

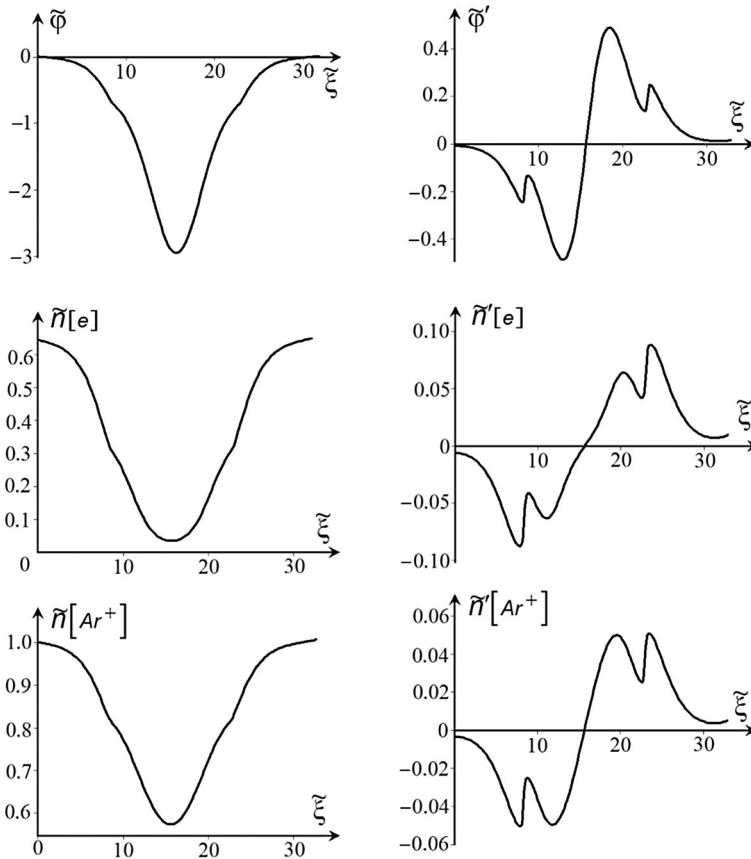


Fig. 23 Profiles of the physical quantities (left) and their first derivatives (right) in the ion-acoustic supersoliton propagating in SF₆–Ar–plasma: electrostatic potential φ (top), electron concentration n_e (middle), and Ar⁺ ion concentration n_{Ar^+} (bottom). The quantities are normalised as $\tilde{\varphi} = -e\varphi/kT_e$, $\tilde{n}_e = n_e/n_{0Ar^+}$, $\tilde{n}_{Ar^+} = n_{Ar^+}/n_{0Ar^+}$, $\tilde{\xi} = \xi\lambda_{De}^{-1}$, where λ_{De} is the electron plasma Debye length (adapted from Dubinov et al. 2012a)

internal separatrices. Variations of the electrostatic potential φ , electron and Ar⁺ ion concentrations, n_e and n_{Ar^+} , and their first derivatives in the detected supersoliton are illustrated in Fig. 23. They are clearly seen to have a wiggling profile shape (left-hand column of Fig. 23) and a non-monotonic behaviour with a few extrema (right-hand column of Fig. 23), typical for the solitary structures observed in the experiments (see Fig. 21).

Such an excellent agreement between the experimental results and their independent theoretical interpretation presented in the current section strongly supports the idea that the ion-acoustic solitary structures of unusual form, detected, in particular, by Nakamura et al. (1985) and Nakamura and Tsukabayashi (1985) in a laboratory four-ion SF₆–Ar–plasma, could be supersolitons with a non-trivial topology of their phase portraits, and a comprehensive search for these structures in multi-component space and astrophysical plasmas is needed.

5 Conclusions

The review addresses current trends in the analysis of a new type of stationary nonlinear waves in multi-species plasmas, periodic super-nonlinear waves (SNW) and solitary super-nonlinear waves (supersolitons), characterised by a non-trivial topology of their phase portraits, long periods, and large amplitudes. The scheme allowing for the classification of these super-nonlinear solutions and their convenient notation is proposed. Using the multi-fluid plasma models, SNWs are shown to have both electrostatic and magnetohydrodynamic nature. The presence of at least three electrically active components in the plasma (e.g. thermal and non-thermal electrons, ions, charged dusty grains, positrons, etc.) is found to be among the essential criteria for the existence of SNWs. In the space plasma context the nearest candidates are an electron–proton plasma penetrated by alpha particles (e.g. typical for the physical conditions of the solar corona and solar wind) and dusty electron–ion plasmas represented in the vast majority of the astrophysical and space objects, which can be expected to support SNW. The increase of the number of plasma species results in a more complicated topology of the SNW's phase portraits, providing a broader set of topologically different SNW types. Alternatively, non-neutral plasma systems with intense beams are also known to support solitary waves (see, e.g. Mo et al. 2013, where the first experimental observation of a KdV-type soliton wave train in electron beams is reported), and thus should be also included into the list of natural plasmas which are expected to sustain supersolitons. First results in this direction have been achieved by Dutta and Sahu (2017), who showed the possibility for the existence of ion-acoustic supersolitons in ion-beam plasmas with stationary dust grains.

So far, periodic SNW and supersolitons have been analytically studied by the mean of the mechanical analogy method based on the Sagdeev pseudopotential representation. One should admit that the application of the perturbation reductive procedures introducing a small parameter into the model for the analysis of these highly nonlinear structures is compromised by their naturally large amplitudes. For instance, neither KdV equation (with the second-order nonlinearity) nor modified KdV equation (third-order nonlinearity) is able to describe supersolitons. In contrast, the Sagdeev pseudopotential technique allows for studying arbitrarily large-amplitude fluctuations, which justifies the choice of it as a conventional tool for the analysis of SNW and supersolitons in *all* considered works. Following its importance in the discussed problem of super-nonlinear waves in plasma, we would like to briefly outline some more aspects behind this approximation, namely the role of the momentum and energy integrals of the governing equations and the role of different sonic Mach numbers in a fully nonlinear analysis is emphasised by McKenzie et al. (2004). This approach should be treated as an alternative to the Sagdeev potential technique, and can be useful in describing spiky wave forms associated with choked flows at the sonic points. The aspects of a Hamiltonian description of the travelling waves in plasma are discussed by Webb et al. (2005) and McKenzie et al. (2007). The role of generalised vorticities and Bernoulli integrals in the formulation of travelling waves in multi-fluid plasmas is studied by

Mace et al. (2007). Webb et al. (2007, 2014) show that there are two different Hamiltonian formulations for the travelling waves, which use the x -momentum integral and the energy integral of the system. The momentum integral can be thought of as the Hamiltonian of the system, in which the variables are constrained by the energy integral. An alternative Hamiltonian formulation also results from using the energy integral as the Hamiltonian in which the momentum integral is a constraint. These formulations are related to the multi-symplectic view of the equations, as developed by, e.g. Bridges (1992), Bridges et al. (2005), Hydon (2005), and Webb et al. (2015).

Typical signatures of SNWs allowing for the detection of them in astrophysical observations and under laboratory conditions are given. More specifically, their oscillation amplitudes are always large (typically greater than or comparable to a non-oscillating background level) and scale with the oscillation periods, while the oscillation profiles are highly anharmonic of a symmetric triangular shape. Furthermore, several observational signals clearly manifesting such a super-nonlinear behaviour and observed in the magnetised plasma of the solar atmosphere, Earth's magnetosphere, in laboratory and numerical experiments are demonstrated. Despite a significant progress in the field, a further comprehensive search for observational evidences of these super-nonlinear structures using modern ground-based and space-borne instruments and experimental plasma machines, and the developing of corresponding analytical models is of the great interest and importance.

Acknowledgements The authors are grateful to Prof. Valery Nakariakov and Prof. George Rowlands for valuable discussions and constructive comments. D.Y. Kolotkov acknowledges the support of the STFC consolidated grant ST/L000733/1. A. E. Dubinov worked in the framework of the Program of Increasing the Competitiveness of NRNU MEPhI.

Compliance with ethical standards

Conflict of interest The authors would like to state that there is no conflict of interest associated with this publication.

References

- L. Abbo, L. Ofman, S.K. Antiochos, V.H. Hansteen, L. Harra, Y.-K. Ko, G. Lapenta, B. Li, P. Riley, L. Strachan, R. von Steiger, Y.-M. Wang, Slow solar wind: observations and modeling. *Space Sci. Rev.* **201**, 55–108 (2016)
- M. Akbari-Moghanjoughi, Double-wells and double-layers in dusty Fermi-Dirac plasmas: Comparison with the semiclassical Thomas-Fermi counterpart. *Phys. Plasmas* **17**(12), 123709 (2010)
- M. Akbari-Moghanjoughi, Universal aspects of localized excitations in graphene. *J. Appl. Phys.* **114**(7), 073302 (2013)
- M. Akbari-Moghanjoughi, Large-amplitude solitons in gravitationally balanced quantum plasmas. *Phys. Plasmas* **21**(8), 082707 (2014)
- M. Ansar Mahmood, S. Mahmood, M. M. Arshad, H. Saleem, Low frequency solitary waves in magnetized electron positron ion plasmas. *Chin. Phys. Lett.* **22**, 632–635 (2005)
- W.I. Axford, J.F. McKenzie, The origin of high speed solar wind streams, in *Solar Wind Seven Colloquium*, ed. by E. Marsch, R. Schwenn (Pergamon Press, Oxford, 1992), pp. 1–5

- T.K. Baluku, M.A. Hellberg, I. Kourakis, N.S. Saini, Dust ion acoustic solitons in a plasma with kappa-distributed electrons. *Phys. Plasmas* **17**(5), 053702 (2010)
- A.R. Barakat, R.W. Schunk, Transport equations for multicomponent anisotropic space plasmas—a review. *Plasma Phys.* **24**, 389–418 (1982)
- R. Bostrom, G. Gustafsson, B. Holback, G. Holmgren, H. Koskinen, Characteristics of solitary waves and weak double layers in the magnetospheric plasma. *Phys. Rev. Lett.* **61**, 82–85 (1988)
- T.J. Bridges, Spatial Hamiltonian Structure, Energy Flux and the Water-Wave Problem. *Proc. R. Soc. Lond. Ser. A* **439**, 297–315 (1992)
- T.J. Bridges, P.E. Hydon, S. Reich, Vorticity and symplecticity in Lagrangian fluid dynamics. *J. Phys. A Math. Gen.* **38**, 1403–1418 (2005)
- R.A. Cairns, A.A. Mamum, R. Bingham, R. Boström, R.O. Dendy, C.M.C. Nairn, P.K. Shukla, Electrostatic solitary structures in non-thermal plasmas. *Geophys. Res. Lett.* **22**, 2709–2712 (1995)
- Y. Chen, Z.-Y. Li, W. Liu, Z.-D. Shi, Solitary kinetic Alfvén waves in the inertial limit region. *Phys. Plasmas* **7**, 371–374 (2000)
- R. Chin, E. Verwichte, G. Rowlands, V.M. Nakariakov, Self-organization of magnetoacoustic waves in a thermally unstable environment. *Phys. Plasmas* **17**(3), 032107 (2010)
- C.R. Choi, D.-Y. Lee, Solitary Alfvén waves in a dusty plasma. *Phys. Plasmas* **14**(5), 052304 (2007)
- C.R. Choi, C.-M. Ryu, D.-Y. Lee, N.C. Lee, Y.-H. Kim, Dust ion acoustic solitary waves in a magnetized dusty plasma with anisotropic ion pressure. *Phys. Lett. A* **364**, 297–303 (2007)
- I.L. Cooney, M.T. Gavin, I. Tao, K.E. Lonngren, A two-dimensional soliton in a positive ion-negative ion plasma. *IEEE Trans. Plasma Sci.* **19**, 1259–1266 (1991a)
- J.L. Cooney, M.T. Gavin, K.E. Lonngren, Radiation of ion acoustic waves in a dispersive positive ion-negative ion plasma. *IEEE Trans. Plasma Sci.* **19**, 545–547 (1991b)
- R.M. Corless, G.H. Gonnet, D.E.G. Hare, D.J. Jeffrey, D.E. Knuth, On the Lambert W function. *Adv. Comput. Math.* **5**, 329–359 (1996)
- R.C. Davidson, *Methods in Nonlinear Plasma Theory* (Academic Press, New York, 1972)
- H.G. Demars, R.W. Schunk, A multi-ion generalized transport model of the polar wind. *J. Geophys. Res.* **99**, 2215–2226 (1994)
- A.E. Dubinov, Gas-dynamic approach in the nonlinear theory of ion acoustic waves in a plasma: an exact solution. *J. Appl. Mech. Tech. Phys.* **48**, 621–628 (2007a)
- A.E. Dubinov, Theory of nonlinear space charge waves in neutralized electron flows: gas-dynamic approach. *Plasma Phys. Rep.* **33**, 210–217 (2007b)
- A.E. Dubinov, On a widespread inaccuracy in defining the mach number of solitons in a plasma. *Plasma Phys. Rep.* **35**, 991–993 (2009)
- A.E. Dubinov, I.D. Dubinova, How can one solve exactly some problems in plasma theory. *J. Plasma Phys.* **71**, 715–728 (2005)
- A.E. Dubinov, D.Y. Kolotkov, Interpretation of ion-acoustic solitons of unusual form in experiments in SF₆–Ar plasma. *High Energy Chem.* **46**, 349–353 (2012a)
- A.E. Dubinov, D.Y. Kolotkov, Ion-acoustic super solitary waves in dusty multispecies plasmas. *IEEE Trans. Plasma Sci.* **40**, 1429–1433 (2012b)
- A.E. Dubinov, D.Y. Kolotkov, Ion-acoustic supersolitons in plasma. *Plasma Phys. Rep.* **38**, 909–912 (2012c)
- A.E. Dubinov, M.A. Sazonkin, Nonlinear adiabatic models of ion-acoustic waves in dust plasma. *J. Tech. Phys.* **53**, 1129–1140 (2008)
- A.E. Dubinov, M.A. Sazonkin, Supernonlinear ion-acoustic waves in a dusty plasma. *Phys. Wave Phenom.* **21**, 118–128 (2013)
- A.E. Dubinov, A.A. Dubinova, M.A. Sazonkin, Nonlinear theory of the isothermal ion-acoustic waves in the warm degenerate plasma. *J. Commun. Technol. Electron.* **55**, 907–920 (2010)
- A.E. Dubinov, D.Y. Kolotkov, M.A. Sazonkin, Nonlinear ion acoustic waves in a quantum degenerate warm plasma with dust grains. *Plasma Phys. Rep.* **37**, 64–74 (2011)
- A.E. Dubinov, D.Y. Kolotkov, M.A. Sazonkin, Supernonlinear waves in plasma. *Plasma Phys. Rep.* **38**, 833–844 (2012)
- I.D. Dubinova, Application of the Lambert W function in mathematical problems of plasma physics. *Plasma Phys. Rep.* **30**, 872–877 (2004)
- D. Dutta, B. Sahu, Nonlinear structures in an ion-beam plasmas including dust impurities with nonthermal nonextensive electrons. *Commun. Theor. Phys.* **68**, 117 (2017)
- D. Dutta, P. Singha, B. Sahu, Interlaced linear-nonlinear wave propagation in a warm multicomponent plasma. *Phys. Plasmas* **21**(12), 122308 (2014)

- M.M. Echim, J. Lemaire, Ø. Lie-Svendsen, A review on solar wind modeling: kinetic and fluid aspects. *Surv. Geophys.* **32**, 1–70 (2011)
- S.A. El-Wakil, E.M. Abulwafa, A.A. Elhanbaly, Super-soliton dust-acoustic waves in four-component dusty plasma using non-extensive electrons and ions distributions. *Phys. Plasmas* **24**(7), 073705 (2017)
- R.E. Ergun, C.W. Carlson, J.P. McFadden, F.S. Mozer, L. Muschietti, I. Roth, R.J. Strangeway, Debye-scale plasma structures associated with magnetic-field-aligned electric fields. *Phys. Rev. Lett.* **81**, 826–829 (1998)
- G.D. Fleishman, A.T. Altyntsev, N.S. Meshalkina, Microwave signature of relativistic positrons in solar flares. *Publ. Astron. Soc. Jpn.* **65**, S7 (2013)
- J.R. Franz, P.M. Kintner, J.S. Pickett, L.-J. Chen, Properties of small-amplitude electron phase-space holes observed by Polar. *J. Geophys. Res. (Space Phys)* **110**, A9212 (2005)
- S.B. Ganguli, The polar wind. *Rev. Geophys.* **34**, 311–348 (1996)
- S.S. Ghosh, G.S. Lakhina, Anomalous width variation of rarefactive ion acoustic solitary waves in the context of auroral plasmas. *Nonlinear Process. Geophys.* **11**, 219–228 (2004)
- S.S. Ghosh, A.N. Sekar Iyengar, Effect of cooler electrons on a compressive ion acoustic solitary wave in a warm ion plasma—forbidden regions, double layers, and supersolitons. *Phys. Plasmas* **21**(8), 082104 (2014)
- M.V. Goldman, M.M. Oppenheim, D.L. Newman, Theory of localized bipolar wave-structures and nonthermal particle distributions in the auroral ionosphere. *Nonlinear Process. Geophys.* **6**, 221–228 (1999)
- G. Gustafsson, M. André, T. Carozzi, A.I. Eriksson, C.-G. Fälthammar, R. Grard, G. Holmgren, J.A. Holtet, N. Ivchenko, T. Karlsson, Y. Khotyaintsev, S. Klimov, H. Laakso, P.-A. Lindqvist, B. Lybekk, G. Marklund, F. Mozer, K. Mursula, A. Pedersen, B. Popielawska, S. Savin, K. Stasiwicz, P. Tanskanen, A. Vaivads, J.-E. Wahlund, First results of electric field and density observations by Cluster EFW based on initial months of operation. *Ann. Geophys.* **19**, 1219–1240 (2001)
- T. Hada, C.F. Kennel, B. Buti, Stationary nonlinear Alfvén waves and solitons. *J. Geophys. Res.* **94**, 65–77 (1989)
- M.A. Hellberg, T.K. Baluku, F. Verheest, I. Kourakis, Dust-acoustic supersolitons in a three-species dusty plasma with kappa distributions. *J. Plasma Phys.* **79**, 1039–1043 (2013)
- N.E. Huang, Z. Wu, A review on Hilbert–Huang transform: method and its applications to geophysical studies. *Rev. Geophys.* **46**, RG2006 (2008)
- N.E. Huang, Z. Shen, S.R. Long, M.C. Wu, H.H. Shih, Q. Zheng, N.-C. Yen, C.C. Tung, H.H. Liu, The empirical mode decomposition and the Hilbert spectrum for nonlinear and non-stationary time series analysis. *Proc. R. Soc. Lond. Ser. A* **454**, 903–998 (1998)
- P.E. Hydon, Multisymplectic conservation laws for differential and differential-difference equations. *Proc. R. Soc. Lond. Ser. A* **461**, 1627–1637 (2005)
- H. Ikezi, Experiments on ion-acoustic solitary waves. *Phys. Fluids* **16**, 1668–1675 (1973)
- E. Infeld, G. Rowlands, *Nonlinear Waves, Solitons and Chaos*, 2nd edn. (Cambridge University Press, Cambridge, 2000)
- P.A. Isenberg, J.V. Hollweg, On the preferential acceleration and heating of solar wind heavy ions. *J. Geophys. Res.* **88**, 3923–3935 (1983)
- I.D. Kaganovich, L.D. Tsendin, Formation of discontinuities in multistage evolution associated with diffusion of a multicomponent weakly ionized hot-electron plasma. *Plasma Phys. Rep.* **19**, 645–650 (1993)
- I.D. Kaganovich, D.J. Economou, B.N. Ramamurthi, V. Midha, Negative ion density fronts during ignition and extinction of plasmas in electronegative gases. *Phys. Rev. Lett.* **84**, 1918–1921 (2000)
- B. Kakad, A. Kakad, Y. Omura, Nonlinear evolution of ion acoustic solitary waves in space plasmas: fluid and particle-in-cell simulations. *J. Geophys. Res. (Space Phys.)* **119**, 5589–5599 (2014)
- A. Kakad, A. Lotekar, B. Kakad, First-ever model simulation of the new subclass of solitons “supersolitons” in plasma. *Phys. Plasmas* **23**(11), 110702 (2016)
- H. Kaur, T. Singh, Gill, Study of large amplitude solitons in multispecies plasma with non-Maxwellian electrons. *J. Phys. Conf. Ser.* **208**(1), 012080 (2010)
- D.Y. Kolotkov, V.M. Nakariakov, G. Rowlands, Nonlinear oscillations of coalescing magnetic flux ropes. *Phys. Rev. E* **93**(5), 053205 (2016)
- I.V. Konikov, O.A. Gorbachev, G.V. Khazanov, A.A. Chernov, Hydrodynamical equations for thermal electrons taking into account their scattering on ion-cyclotron waves in the outer plasmasphere of the earth. *Planet. Space Sci.* **37**, 1157–1168 (1989)

- H.H. Kuehl, K. Imen, Ion-acoustic solitary waves near double layers. *IEEE Trans. Plasma Sci.* **13**, 37–40 (1985)
- G.S. Lakhina, S.V. Singh, A.P. Kakad, Ion acoustic solitons/double layers in two-ion plasma revisited. *Phys. Plasmas* **21**(6), 062311 (2014)
- I. Lopes, D. Passos, M. Nagy, K. Petrovay, Oscillator models of the solar cycle. Towards the development of inversion methods. *Space Sci. Rev.* **186**, 535–559 (2014)
- A. Lotekar, A. Kakad, B. Kakad, Fluid simulation of dispersive and nondispersive ion acoustic waves in the presence of superthermal electrons. *Phys. Plasmas* **23**(10), 102108 (2016)
- Q.M. Lu, D.Y. Wang, S. Wang, Generation mechanism of electrostatic solitary structures in the Earth's auroral region. *J. Geophys. Res. (Space Phys.)* **110**, A3223 (2005)
- G.O. Ludwig, J.L. Ferreira, Y. Nakamura, Observation of ion-acoustic rarefaction solitons in a multicomponent plasma with negative ions. *Phys. Rev. Lett.* **52**, 275–278 (1984)
- R.L. Mace, J.F. McKenzie, G.M. Webb, Conservation laws for steady flow and solitons in a multicomponent plasma revisited. *Phys. Plasmas* **14**(1), 012310 (2007)
- S.K. Maharaj, R. Bharuthram, S.V. Singh, G.S. Lakhina, Existence domains of dust-acoustic solitons and supersolitons. *Phys. Plasmas* **20**(8), 083705 (2013)
- A.A. Mamun, P.K. Shukla, Arbitrary amplitude solitary waves and double layers in an ultra-relativistic degenerate dense dusty plasma. *Phys. Lett. A* **374**, 4238–4241 (2010)
- W. Masood, H.A. Shah, N.L. Tsintsadze, M.N.S. Qureshi, Dust Alfvén ordinary and cusp solitons and modulational instability in a self-gravitating magneto-radiative plasma. *Eur. Phys. J. D* **59**, 413–419 (2010)
- J.F. McKenzie, E. Dubinin, K. Sauer, T.B. Doyle, The application of the constants of motion to nonlinear stationary waves in complex plasmas: a unified fluid dynamic viewpoint. *J. Plasma Phys.* **70**, 431–462 (2004)
- J.F. McKenzie, R.L. Mace, T.B. Doyle, Nonlinear Hall MHD and electrostatic ion-cyclotron stationary waves: a Hamiltonian-geometric viewpoint. *J. Plasma Phys.* **73**, 687–700 (2007)
- C.A. Mendoza-Briceño, S.M. Russel, A.A. Mamun, Large amplitude electrostatic solitary structures in a hot non-thermal dusty plasma. *Planet. Space Sci.* **48**, 599–608 (2000)
- Y.C. Mo, R.A. Kishek, D. Feldman, I. Haber, B. Beaudoin, P.G. O'Shea, J.C.T. Thangaraj, Experimental observations of soliton wave trains in electron beams. *Phys. Rev. Lett.* **110**(8), 084802 (2013)
- F.S. Mozer, R. Ergun, M. Temerin, C. Cattell, J. Dombeck, J. Wygant, New features of time domain electric-field structures in the auroral acceleration region. *Phys. Rev. Lett.* **79**, 1281–1284 (1997)
- K. Murawski, Stability of modified Korteweg-de Vries waves. *Aust. J. Phys.* **40**, 593–599 (1987)
- R.J. Murphy, B. Kozlovsky, G.H. Share, Radioactive positron emitter production by energetic alpha particles in solar flares. *Astrophys. J. Suppl.* **215**, 18 (2014)
- Y. Nakamura, Experiments on ion-acoustic solitons in plasmas. *IEEE Trans. Plasma Sci.* **10**, 180–195 (1982)
- Y. Nakamura, I. Tsukabayashi, Modified Korteweg-de Vries ion-acoustic solitons in a plasma. *J. Plasma Phys.* **34**, 401–415 (1985)
- Y. Nakamura, J.L. Ferreira, G.O. Ludwig, Experiments on ion-acoustic rarefactive solitons in a multicomponent plasma with negative ions. *J. Plasma Phys.* **33**, 237–248 (1985)
- V.M. Nakariakov, V.F. Melnikov, Quasi-periodic pulsations in solar flares. *Space Sci. Rev.* **149**, 119–151 (2009)
- V.M. Nakariakov, E. Verwichte, Coronal waves and oscillations. *Living Rev. Sol. Phys.* **2**, 3–65 (2005)
- V.M. Nakariakov, A.R. Inglis, I.V. Zimovets, C. Foullon, E. Verwichte, R. Sych, I.N. Myagkova, Oscillatory processes in solar flares. *Plasma Phys. Control. Fusion* **52**(12), 124009 (2010)
- V.M. Nakariakov, V. Pilipenko, B. Heilig, P. Jelínek, M. Karlický, D.Y. Klimushkin, D.Y. Kolotkov, D.-H. Lee, G. Nisticò, T. Van Doorselaere, G. Verth, I.V. Zimovets, Magnetohydrodynamic oscillations in the solar corona and Earth's magnetosphere: towards consolidated understanding. *Space Sci. Rev.* **200**, 75–203 (2016)
- C.P. Olivier, S.K. Maharaj, R. Bharuthram, Ion-acoustic solitons, double layers and supersolitons in a plasma with two ion- and two electron species. *Phys. Plasmas* **22**(8), 082312 (2015)
- C.P. Olivier, F. Verheest, S.K. Maharaj, Small-amplitude supersolitons near supercritical plasma compositions. *J. Plasma Phys.* **83**(4), 905830403 (2017)
- D.J. Pascoe, C.R. Goddard, G. Nisticò, S. Anfinogentov, V.M. Nakariakov, Damping profile of standing kink oscillations observed by SDO/AIA. *Astron. Astrophys.* **585**, L6 (2016)
- A. Paul, A. Bandyopadhyay, Dust ion acoustic solitary structures in presence of nonthermal electrons and isothermal positrons. *Astrophys. Space Sci.* **361**, 172 (2016)

- I. Paul, S. Chandra, S. Chattopadhyay, S.N. Paul, W-type ion-acoustic solitary waves in plasma consisting of cold ions and nonthermal electrons. *Indian J. Phys.* **90**, 1195–1205 (2016)
- S.I. Popel, A.A. Gisko, Charged dust and shock phenomena in the solar system. *Nonlinear Process. Geophys.* **13**, 223–229 (2006)
- O.R. Rufai, Auroral electrostatic solitons and supersolitons in a magnetized nonthermal plasma. *Phys. Plasmas* **22**(5), 052309 (2015)
- O.R. Rufai, R. Bharuthram, S.V. Singh, G.S. Lakhina, Ion acoustic solitons and supersolitons in a magnetized plasma with nonthermal hot electrons and Boltzmann cool electrons. *Phys. Plasmas* **21**(8), 082304 (2014)
- O.R. Rufai, R. Bharuthram, S.V. Singh, G.S. Lakhina, Effect of excess superthermal hot electrons on finite amplitude ion-acoustic solitons and supersolitons in a magnetized auroral plasma. *Phys. Plasmas* **22**(10), 102305 (2015)
- O.R. Rufai, R. Bharuthram, S.V. Singh, G.S. Lakhina, Nonlinear low frequency electrostatic structures in a magnetized two-component auroral plasma. *Phys. Plasmas* **23**(3), 032309 (2016a)
- O.R. Rufai, R. Bharuthram, S.V. Singh, G.S. Lakhina, Obliquely propagating ion-acoustic solitons and supersolitons in four-component auroral plasmas. *Adv. Space Res.* **57**, 813–820 (2016b)
- N.M. Ryskin, D.I. Trubetskoy, *Nonlinear Waves* (Fizmatlit, Moscow, 2000) (in Russian)
- R.W. Schunk, Mathematical structure of transport equations for multispecies flows. *Rev. Geophys. Space Phys.* **15**, 429–445 (1977)
- G.H. Share, R.J. Murphy, D.M. Smith, R.A. Schwartz, R.P. Lin, RHESSI e^+e^- annihilation radiation observations: implications for conditions in the flaring solar chromosphere. *Astrophys. J. Lett.* **615**, L169–L172 (2004)
- S.V. Singh, G.S. Lakhina, Ion-acoustic supersolitons in the presence of non-thermal electrons. *Commun. Nonlinear Sci. Numer. Simul.* **23**, 274–281 (2015)
- B.M. Smirnov, Physics of ball lightning. *Phys. Rep.* **224**, 151–236 (1993)
- S.V. Steffy, S.S. Ghosh, Existence domain of the compressive ion acoustic super solitary wave in a two electron temperature warm multi-ion plasma. *Phys. Plasmas* **24**(10), 102111 (2017)
- W. Swider, Electron loss and the determination of electron concentrations in the D-region. *Pure Appl. Geophys.* **127**, 403–414 (1988)
- W. Swider, Sodium chemistry—a brief review and two new mechanisms for sudden sodium layers. *Planet. Space Sci.* **40**, 247–253 (1992)
- T. Takeuchi, S. Iizuka, N. Sato, Ion acoustic shocks formed in a collisionless plasma with negative ions. *Phys. Rev. Lett.* **80**, 77–80 (1998)
- R.J. Taylor, K.R. MacKenzie, H. Ikezi, A large double plasma device for plasma beam and wave studies. *Rev. Sci. Instrum.* **43**, 1675–1678 (1972)
- M. Temerin, K. Cerny, W. Lotko, F.S. Mozer, Observations of double layers and solitary waves in the auroral plasma. *Phys. Rev. Lett.* **48**, 1175–1179 (1982)
- C.-Y. Tu, A solar wind model with the power spectrum of Alfvénic fluctuations. *Solar Phys.* **109**, 149–186 (1987)
- C.-Y. Tu, E. Marsch, Two-fluid model for heating of the solar corona and acceleration of the solar wind by high-frequency Alfvén waves. *Solar Phys.* **171**, 363–391 (1997)
- S.R. Valluri, D.J. Jeffrey, R.M. Corless, Tutorial/Article didactique: some applications of the Lambert W function to physics. *Can. J. Phys.* **78**, 823 (2000)
- T. Van Doorselaere, E.G. Kupriyanova, D. Yuan, Quasi-periodic pulsations in solar and stellar flares: an overview of recent results. *Sol. Phys.* **291**, 3143–3164 (2016)
- I.Y. Vasko, O.V. Agapitov, F. Mozer, A.V. Artemyev, D. Jovanovic, Magnetic field depression within electron holes. *Geophys. Res. Lett.* **42**, 2123–2129 (2015)
- F. Verheest, Nonlinear acoustic waves in nonthermal plasmas with negative and positive dust. *Phys. Plasmas* **16**(1), 013704 (2009)
- F. Verheest, Dust-acoustic solitary modes in plasmas with isothermal and nonthermal ions: Polarity switches and coexistence domains. *Phys. Plasmas* **18**(8), 083701 (2011)
- F. Verheest, Electrostatic nonlinear supersolitons in dusty plasmas. *J. Plasma Phys.* **80**, 787–793 (2014)
- F. Verheest, M.A. Hellberg, Electrostatic supersolitons and double layers at the acoustic speed. *Phys. Plasmas* **22**(1), 012301 (2015)
- F. Verheest, M.A. Hellberg, G.J. Gray, R.L. Mace, Electrostatic solitons in multispecies electron–positron plasmas. *Astrophys. Space Sci.* **239**, 125–139 (1996)
- F. Verheest, M.A. Hellberg, I. Kourakis, Dust-ion-acoustic supersolitons in dusty plasmas with nonthermal electrons. *Phys. Rev. E* **87**(4), 043107 (2013a)

- F. Verheest, M.A. Hellberg, I. Kourakis, Electrostatic supersolitons in three-species plasmas. *Phys. Plasmas* **20**(1), 012302 (2013b)
- F. Verheest, M.A. Hellberg, I. Kourakis, Ion-acoustic supersolitons in plasmas with two-temperature electrons: Boltzmann and kappa distributions. *Phys. Plasmas* **20**(8), 082309 (2013c)
- F. Verheest, G.S. Lakhina, M.A. Hellberg, No electrostatic supersolitons in two-component plasmas. *Phys. Plasmas* **21**(6), 062303 (2014)
- G.M. Webb, J.F. McKenzie, E.M. Dubinin, K. Sauer, Hamiltonian formulation of nonlinear travelling Whistler waves. *Nonlinear Process. Geophys.* **12**, 643–660 (2005)
- G.M. Webb, J.F. McKenzie, R.L. Mace, C.M. Ko, G.P. Zank, Dual variational principles for nonlinear traveling waves in multifluid plasmas. *Phys. Plasmas* **14**(8), 082318 (2007)
- G.M. Webb, C.M. Ko, R.L. Mace, J.F. McKenzie, G.P. Zank, Integrable, oblique travelling waves in quasi-charge-neutral two-fluid plasmas. *Nonlinear Process. Geophys.* **15**, 179–208 (2008)
- G.M. Webb, R.H. Burrows, X. Ao, G.P. Zank, Ion acoustic traveling waves. *J. Plasma Phys.* **80**, 147–171 (2014)
- G.M. Webb, J.F. McKenzie, G.P. Zank, Multi-symplectic magnetohydrodynamics: II, addendum and erratum. *J. Plasma Phys.* **81**(6), 905810610 (2015)
- M.Y. Yu, H. Luo, A note on the multispecies model for identical particles. *Phys. Plasmas* **15**(2), 024504 (2008)